ANNUAL REVIEWS

Annual Review of Astronomy and Astrophysics

The Evolution of Massive Binary Stars

Pablo Marchant[1] and Julia Bodensteiner[2]

[1]Institute of Astronomy, KU Leuven, Leuven, Belgium; email: pablo.marchant@kuleuven.be

[2]European Organisation for Astronomical Research in the Southern Hemisphere (ESO), Garching, Germany; email: julia.bodensteiner@eso.org

Annu. Rev. Astron. Astrophys. 2024. 62:21–61

First published as a Review in Advance on April 19, 2024

The *Annual Review of Astronomy and Astrophysics* is online at astro.annualreviews.org

https://doi.org/10.1146/annurev-astro-052722-105936

Keywords

massive stars, stellar evolution, rotation, compact objects, gravitational waves

Abstract

Massive stars play a major role in the evolution of their host galaxies and serve as important probes of the distant Universe. It has been established that the majority of massive stars reside in close binaries and interact with their companion stars during their lifetimes. Such interactions drastically alter their life cycles and complicate our understanding of their evolution, but are also responsible for the production of interesting and exotic interaction products.

- Extensive observation campaigns with well-understood detection sensitivities have enabled the conversion of observed properties into intrinsic characteristics, facilitating a direct comparison to theory.
- Studies of large samples of massive stars in our Galaxy and the Magellanic Clouds have unveiled new types of interaction products, providing critical constraints on the mass transfer phase and the formation of compact objects.
- The direct detection of gravitational waves has revolutionized the study of stellar mass compact objects, providing a new window to study massive star evolution. Their formation processes are, however, still unclear. The known sample of compact object mergers will increase by orders of magnitude in the coming decade, which is vastly outgrowing the number of stellar-mass compact objects detected through electromagnetic radiation.

Contents

1. INTRODUCTION

Massive stars are powerful cosmic engines, capable of modifying their local, galactic and even extragalactic environments (Hopkins et al. 2014). Through their high luminosities, which can include a significant fraction of ionizing radiation, they are understood to play a critical role in the reionization of the Universe (Haiman & Loeb 1997). Radiation-driven stellar winds can remove large fractions of the stellar birth mass (Vink 2022), providing kinetic feedback and chemically processed matter. At the end of their lives, energetic supernova (SN) explosions further enrich their surroundings with matter that has undergone late nuclear burning stages (Nomoto et al. 2013), acting as one of the main drivers of the chemical evolution of galaxies. Although rare objects, massive stars dominate the integrated light of distant galaxies (e.g., Pettini et al. 2000). Yet, despite their broad astrophysical importance, various physical processes that dominate their evolution are still largely uncertain (see Langer 2012 for a recent review).

One critical aspect that undermines the understanding of massive stars is their scarcity. In the local Universe, $<1\%$ of stars born are expected to be massive (Kroupa 2002), which is further compounded by their orders-of-magnitude shorter lifetimes compared to intermediate- and low-mass stars. But another critical complication arises from the prevalence of close binaries in massive stars. For several decades, multiepoch spectroscopic observations have indicated that a large fraction of massive stars have close binary companions (Levato et al. 1987, Abt et al. 1990, Kobulnicky & Fryer 2007). By carefully accounting for observational biases, it has been shown that the majority of massive stars undergo interaction phases that dominate their evolution, potentially with over half of them interacting before the end of the main sequence (MS; Sana et al. 2012). Detections made through photometry, astrometry, or other techniques that cover different regimes not accessible by spectroscopy further indicate that a large number of stars have multiple companions (see Moe & Di Stefano 2017 for a recent compilation). Binary evolution adds on the complexity of massive-star physics, providing a rich set of postinteraction products such as stripped stars (Shenar et al. 2020a, Drout et al. 2023), rapidly rotating accretors (de Mink et al. 2013, Renzo & Götberg 2021), mergers (Schneider et al. 2019, Hirai et al. 2021), exotic SNe (Chevalier 2012, Metzger 2022), X-ray binaries (Tauris & van den Heuvel 2006, Gilfanov et al. 2023), and double-degenerate binaries, which may produce detectable gravitational wave (GW) emissions (Tauris et al. 2017, Mandel & Farmer 2022). Observations of apparently single stars can hide a past of binary interaction, leading to the erroneous attribution of their physical properties to single-star physics (de Mink et al. 2014).

Even if theory can describe the intrinsic properties of a given stellar population, comparison to observations requires a clear understanding of the biases involved in sample selection and instrumental limitations. Large-scale surveys with clearly defined selection criteria play a critical role in this regard. This is the case for spectroscopic surveys such as the VLT-FLAMES Tarantula Survey (VFTS; for an overview see Evans et al. 2011), photometric surveys like those from *Kepler* (Borucki et al. 2010, Koch et al. 2010) and the *Transiting Exoplanet Survey Satellite* (TESS; Ricker et al. 2015), and astrometric measurements of the *Gaia* mission (Gaia Collab. et al. 2016). Entire populations of high-mass X-ray binaries (HMXBs) can be probed in individual galaxies with X-ray observations (Gilfanov et al. 2023). Transient observations through multiband synoptic surveys have also provided breakthroughs in our understanding of SNe. For instance, the Zwicky Transient Facility (Bellm et al. 2019) currently produces on the order of a million daily transient alerts, with dedicated infrastructure to perform spectroscopic follow-up and classification of the brightest ones (Fremling et al. 2020). However, the most significant development in the past decade did not involve electromagnetism, but rather the direct detection of GWs from merging compact objects (Abbott et al. 2016). Ground-based interferometers such as the Laser Interferometer Gravitational-Wave Observatory (LIGO; Aasi et al. 2015) and Virgo (Acernese et al. 2015) have well-understood biases, making it straightforward to determine intrinsic population properties or to apply biases synthetically to predicted populations.

Owing to the great progress seen in the past decade, a review of the current state of and outstanding problems in the field of massive binary evolution is of critical importance. However, a full comprehensive review is not possible within the scope of this document, and as such, our focus is on progress made since the review by Langer (2012) on single and binary massive-star evolution. We avoid overlap with the recent reviews by Eldridge & Stanway (2022) on the impact of massive binaries on the evolution of early galaxies, Kaaret et al. (2017) on ultraluminous X-ray sources (ULXs), and Murase & Bartos (2019) on multimessenger astrophysics. We also exclude from the discussion the evolution of low-mass X-ray binaries, whose formation is potentially affected by stellar dynamics (e.g., Ivanova et al. 2010). The field of transients and SNe associated with binary evolution is also rapidly growing, and cannot be comprehensively covered in this review (for a recent overview, see Tauris & van den Heuvel 2023, their chapter 13). However, we soften the definition of "massive star"[1] and include findings for intermediate-mass stars when relevant in the massive-star regime.

The outline of this review is as follows: In Section 2, we discuss the different spatial and temporal scales of interacting binaries. In Section 3, we report the observational constraints on binary fractions and orbital parameters at different evolutionary stages. In Section 4, we review the main binary interaction processes, and discuss the theoretical tools used to model them. We then describe the properties of nondegenerate postinteraction products in Section 5, and how their observation constrains our theoretical models. In Section 6, we discuss the properties of single- and double-degenerate interaction products. In Section 7, we provide a brief overview on the observations of GW sources and their potential formation through binary evolution. Finally, we conclude in Section 8.

Mass ratio, q: often defined as $q = m_{\rm donor}/m_{\rm accretor}$ or its inverse; it is always best to specify the definition used

Case A: mass transfer phase initiated during the main sequence of the donor star

Case B: mass transfer phase initiated after the main sequence and before core helium depletion of the donor star

Case C: mass transfer phase initiated after core helium depletion of the donor star

2. THE SCALES OF BINARY INTERACTION

Whether or not the components in a binary system interact, and what type of interactions occur, is mainly dictated by the radial evolution of both stars. As a star evolves, it can eventually fill its Roche lobe, producing outflows through the first Lagrangian point L1 toward its companion. In binary evolution models, Roche lobes are approximated by a volume-equivalent radius, normally computed through the fit made by Eggleton (1983) in terms of the mass ratio ($q \equiv m_1/m_2$):

$$R_{\rm RL,1}(q) = f(q)a, \quad f(q) = \frac{0.49q^{2/3}}{0.6q^{2/3} + \ln(1 + q^{1/3})}, \qquad 1.$$

where $R_{\rm RL,1}$ is the Roche lobe radius of the star with mass m_1, and a is the orbital separation. Even if a star does not fill its Roche lobe, interactions can still happen through tidal effects, wind-orbit coupling, and irradiation. On the opposite extreme, binary stars can extend well beyond the L1 point, in either stable contact systems or dynamically evolving common envelope (CE) configurations.

Roche lobe overflow (RLOF) is the most transformative form of interaction in binaries. Following the work of Kippenhahn & Weigert (1967), phases of mass transfer are nominated as Cases (capitalized for historical reasons). Case A mass transfer refers to RLOF episodes during the MS of the donor star, whereas Case B mass transfer refers to RLOF before core helium depletion. Case B is often split into early and late Case B, indicating interaction before or after the development of a convective envelope. Case C mass transfer corresponds to late interactions post core helium depletion (Lauterborn 1970). Note that these definitions can be inconsistent in the literature, with Case B and Case C instead representing mass transfer before and after the ignition of helium, respectively (Podsiadlowski et al. 1992). Repeated interactions are marked with multiple letters, such that Case AB refers to a mass transfer event after the MS, which was preceded by Case A mass transfer.

The range in separations and orbital periods at which RLOF is expected is illustrated[2] in **Figure 1**. As massive stars can expand by over two orders of magnitude, RLOF can occur at orbital separations ranging from tens of solar radii up to about ten astronomical units (for mass

[1]Langer (2012, p. 108) defined a massive star as "a star that is massive enough to form a collapsing core at the end of its life and, thus, avoid the white dwarf fate."

[2]All stellar evolution tracks shown in this review were computed using the `MESA` stellar evolution code at solar metallicity ($Z = 0.0142$; Asplund et al. 2009). All data needed to reproduce our figures and simulations are provided at **https://doi.org/10.5281/zenodo.10009234**.

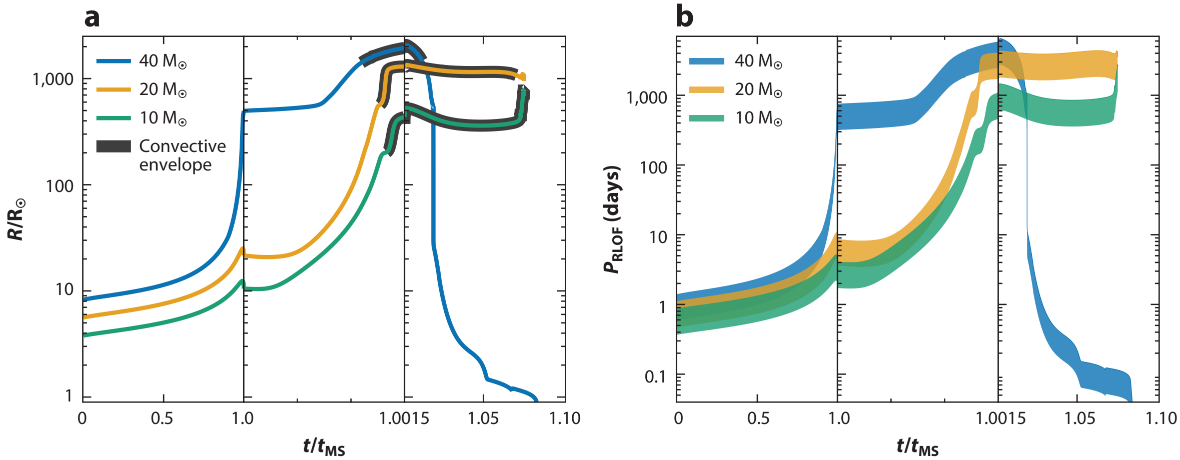

Figure 1

(*a*) Radial evolution of massive stars at solar metallicity with different masses (see legend) as a function of time in units of the MS lifetime. The thick black line indicates points at which the star develops a convective envelope containing more than 10% of the total mass. (*b*) Range of orbital periods (considering an arbitrary mass ratio) for which these stars would undergo RLOF. Abbreviations: MS, main sequence; RLOF, Roche lobe overflow.

ratios of order unity). For a given stellar radius R_1, the period at which RLOF occurs is given by

$$P_{\rm RLOF} = R_1^{3/2}\left(\frac{4\pi^2}{Gm_1}\right)^{1/2} g(q), \quad g(q) \equiv (f(q))^{-3/2}\left(\frac{q}{1+q}\right)^{1/2}. \qquad 2.$$

The function $g(q)$ is bound between 3.3 and 1.35, resulting in a finite range of periods for which a star would undergo RLOF, independent of the mass ratio. As shown in **Figure 1*a***, solar-metallicity massive stars are expected to undergo RLOF at the zero-age MS for periods of ∼1 day, whereas at their maximum expansion they can undergo RLOF at periods of ∼10 years. As such, interacting binary systems operate over a large range of spatial and temporal timescales.

Orbital evolution can be computed in terms of the orbital angular momentum,

$$J = m_1 m_2 \sqrt{\frac{Ga(1-e^2)}{m_1+m_2}}. \qquad 3.$$

It is common to assume near-RLOF systems to be efficiently circularized (e.g., Verbunt & Phinney 1995), in which case the time derivative of the orbital angular momentum is

$$\frac{\dot{J}}{J} = \frac{\dot{m}_1}{m_1} + \frac{\dot{m}_1}{m_2} - \frac{1}{2}\frac{\dot{m}_1+\dot{m}_2}{m_1+m_2} + \frac{1}{2}\frac{\dot{a}}{a}. \qquad 4.$$

Having a model for how the masses of a binary system evolve with time and how angular momentum is removed or added to the orbit allows for the integration of this equation to determine the evolution of the orbital separation. For some simple models, the evolution of the separation as a function of the component masses can be determined analytically, serving as a useful probe to determine the future outcome of a binary observed pre-RLOF or to understand the potential progenitors of a postinteraction system (see, e.g., Soberman et al. 1997, Tauris & van den Heuvel 2023). The detailed dynamics of binary outflows and the angular momentum they remove remains an important uncertainty in evolutionary calculations (e.g., Brookshaw & Tavani 1993, MacLeod & Loeb 2020, Willcox et al. 2023).

3. CONSTRAINTS ON BINARITY AT DIFFERENT EVOLUTIONARY STAGES

A consensus that massive stars are predominantly part of binary or higher-order multiple systems has been established over the past few decades using a multitude of different observations and detection techniques. They probe different regions of the parameter space and suffer from different observational biases and limitations.

Photometric signatures such as eclipses and ellipsoidal variations can be detected in the closest, shortest-period binaries if their orientation toward the observer is favorable. Spectroscopic observations mainly use radial velocity (RV) variations to detect binaries and constrain orbital parameters such as the period and eccentricity in the case of single-lined spectroscopic binaries (SB1s), where only one component, usually denoted as primary, is visible. Additionally, the mass ratio (often defined as the mass of the less luminous star, the secondary, over the mass of the primary) can be measured in double-lined spectroscopic binaries (SB2s), where the signature of both stars appears in the spectrum. Spectroscopic observations probe orbital periods that are of the order of the length of the observing campaign (usually up to a few years) but suffer from severe observational biases depending on the system's parameters and orientation (e.g., Sana et al. 2012; see also Section 3.1).

Long-baseline interferometry, which is still technically feasible only for brighter stars in our Galaxy with current instrumentation, allows for probing binary systems that have angular separations between ∼1 and 100 mas, corresponding to orbital periods on the order of months to decades for Galactic distances (e.g., Sana et al. 2014, Le Bouquin et al. 2017, GRAVITY Collab. et al. 2018, Bordier et al. 2022, Lanthermann et al. 2023). Similarly, high-precision long-term astrometric monitoring allows the detection of wider binaries. While barely any orbital solutions for massive stars are included in the third *Gaia* data release (DR3) (Gaia Collab. et al. 2021; see also Section 6.3), the fourth *Gaia* data release (DR4), expected toward the end of 2025, should improve this situation significantly by providing orbital constraints for a large number of massive binaries. Scales between ∼10 and 1,000 mas were probed with the fine guidance sensor of the *Hubble Space Telescope* (e.g., Aldoretta et al. 2015). Binaries with even larger separations or more distant companions in higher-order multiples (with angular separations of ∼100–10,000 mas) can further be detected with high angular resolution imaging techniques such as high-contrast or AO (adaptive optics)-supported imaging (e.g., Mason et al. 2009, Sana et al. 2014, Rainot et al. 2020, Kalari et al. 2022, Reggiani et al. 2022, Pauwels et al. 2023).

As binary interactions are thought to occur in close binaries with periods below ∼10 years (e.g., Podsiadlowski et al. 1992; see Section 2), we focus on spectroscopic surveys in the following and only briefly mention complementary observations using other techniques. Thereby, we go through different evolutionary stages, from the MS to evolved stars. A schematic overview of reported binary properties across the Hertzsprung–Russell diagram (HRD) is displayed in **Figure 2**; references are given in the text.

3.1. OB Stars

Several spectroscopic studies targeting the multiplicity properties of OB stars at different metallicity were performed in recent years (for an overview, see **Table 1**). As most interactions occur after the MS when the primary expands (see Section 2), the observed properties of OB binaries are often considered as initial conditions and serve as input for other fields, such as population synthesis computations (Eldridge et al. 2017) or GW progenitor studies (de Mink & Belczynski 2015). Multiplicity properties studied in the field as well as in cluster environments are described below.

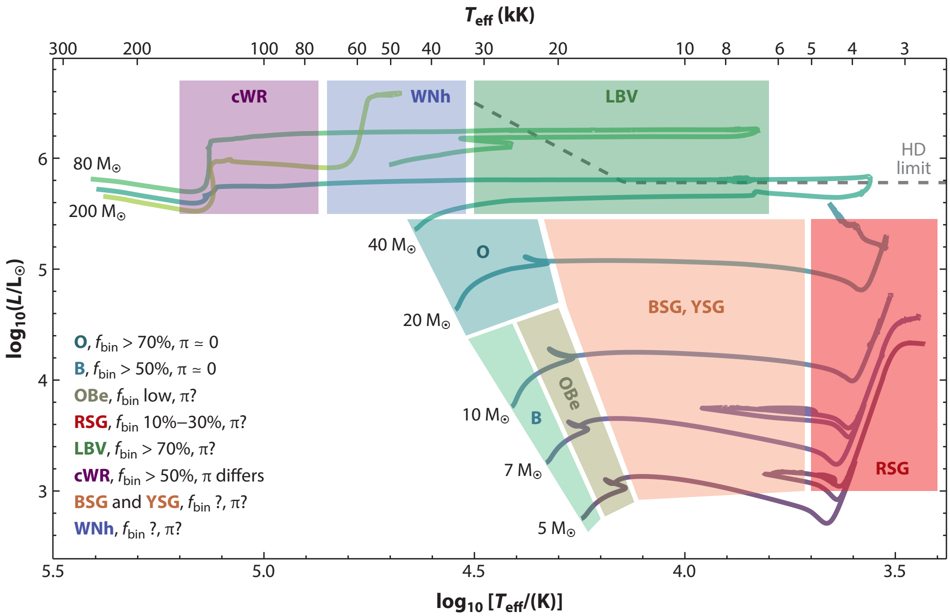

Figure 2

Binary fractions and the index of the period distribution π [which describes a period distribution $dN/d\log P \propto (\log P)^\pi$] for different classes of stars and evolutionary stages across the HRD. Stellar evolution tracks are shown covering evolution from the zero-age MS until core-carbon depletion (or until just before the hydrogen envelope is removed in the AGB phase for the 5-$M_\odot$ and 7-$M_\odot$ models). The HD limit, above which there is a lack of observed stars is indicated with a dashed line (data taken from Humphreys & Davidson 1979). Boxes indicate schematic locations of different types of stars. Abbreviations: AGB, asymptotic giant branch; BSG, blue supergiant; cWR, classical Wolf–Rayet; HD, Humphreys–Davidson; HRD, Hertzsprung–Russell diagram; LBV, luminous blue variable; MS, main sequence; RSG, red supergiant; WNh, nitrogen-rich Wolf–Rayet with hydrogen lines; YSG, yellow supergiant.

Large magnitude-limited surveys of Galactic OB stars in the field in both the Northern and Southern Hemispheres such as IACOB or OWN showed that the observed binary fraction of O-type stars is around 55–65% (Abt et al. 1990, Sota et al. 2014, Barbá et al. 2017, Britavskiy et al. 2019). For B-stars in the field, the observed binary fraction was claimed to decrease down to 45–20% for early to late B-type stars, respectively, based on line profile variations (Chini et al. 2012). In the Small Magellanic Cloud (SMC), the multiepoch spectroscopic RIOTS survey of OB stars reported an observed binary fraction of 59 ± 12% (excluding OBe stars; Lamb et al. 2016).

The results described above for observed binary fractions of field OB stars in the Galaxy are consistent with spectroscopic surveys of OB stars in young Galactic clusters (Sana et al. 2012, Kobulnicky et al. 2014, Banyard et al. 2022). Although those surveys target only a specific region, they can be considered volume-limited samples as all stars are at a similar distance. The VFTS of the 30 Doradus star-forming complex in the Large Magellanic Cloud (LMC; Evans et al. 2011, Sana et al. 2013, Dunstall et al. 2015) measured lower observed binary fractions of $25 \pm 2\%$ to $35 \pm 3\%$ for early-B- and O-type stars. This is similar to the observed binary fraction measured in the young cluster NGC 346 in the SMC (Dufton et al. 2019). Based on low-resolution spectroscopy, the observed binary fraction in NGC 330, a slightly older cluster in the SMC, was found to be even lower with only ∼13 ± 2% (Bodensteiner et al. 2020a).

Binary fraction, f_{bin}: $f_{bin} = N_B/N$, with N_B being the number of binaries (either observed or intrinsic) and N the number of objects

In principle, observed binary fractions give a lower limit on the intrinsic fractions. However, observed fractions are not directly comparable as different observing campaigns use different

Table 1 Spectroscopic surveys of OB stars investigating binarity[a]

n_*	Age (Myr)	Spectral type	f_{bin}^{obs} (%)	f_{bin}^{intr} (%)	P_{max} (days)	Survey	Environment	Reference
Milky Way								
205	?	O&WN	55 ± 3	–		OWN	Southern Hem.	Barbá et al. 2017
194	?	O	65 ± 3	–		GOSSS	Mixed	Sota et al. 2014
319	?	O	43 ± 3[b]	–		IACOB	Northern Hem.	Britavskiy et al. 2023
243	?	O	68 ± 3	–		BESOS	Mixed	Chini et al. 2012
226	?	early-B	46 ± 3	–		BESOS	Mixed	Chini et al. 2012
353	?	late-B	19 ± 2	–		BESOS	Mixed	Chini et al. 2012
74	?	B2–B5	35 ± 4	–			Mixed	Abt et al. 1990
71	1–4	O3-O9.7	56 ± 6	69 ± 9	3,000		Cluster[c]	Sana et al. 2012
7	2–3	O4-O8 I+	$\gtrsim$29	–	–	Arches	Cluster	Clark et al. 2023
13	2–3	WNLha	$\gtrsim$62	–	–	Arches	Cluster	Clark et al. 2023
80	2–7	B0-B9	33 ± 5	52 ± 8[d]	3,000	NGC 6231	Cluster	Banyard et al. 2022
128	3–4	OB	51 ± 7	∼55	5,000	Cyg OB2	Association	Kobulnicky et al. 2014
81	10–5	B	39 ± 9	–	100	Sco OB2	Association	Levato et al. 1987
LMC								
360	5–15	O	35 ± 3	51 ± 4	3,000	30 Dor	SF complex	Sana et al. 2013
408	5–15	early-B	25 ± 2	58 ± 11	3,000	30 Dor	SF complex	Dunstall et al. 2015
SMC								
17	?	OB	59 ± 12	–	–	RIOTS	SMC field	Lamb et al. 2016
47	∼2	O	26 ± 6	–		NGC 346	Cluster	Dufton et al. 2019
288	∼2	B	18 ± 2	–		NGC 346	Cluster	Dufton et al. 2019
284	35–40	B	13 ± 2	34^{+8}_{-7}[d]	3,000	NGC 330	Cluster	Bodensteiner et al. 2021

Abbreviations: Hem., Hemisphere; LMC, Large Magellanic Cloud; SB1, single-lined spectroscopic binary; SB2, double-lined spectroscopic binary; SF, star formation; SMC, Small Magellanic Cloud.

[a]The columns give the number of observed stars, n_*; the age of the population for clusters and associations; the observed (f_{bin}^{obs}) and bias-corrected (f_{bin}^{intr}) spectroscopic binary fractions; the period, P_{max}, up to which the observational biases are corrected for; the name of the survey; the environment; and the relevant reference. Rows are grouped by host galaxy. For field populations, ages are marked with a question mark (?) to indicate that their ages are unconstrained. Properties marked with a dash (–) indicate that this was not derived in the corresponding work.

[b]We here combine the fractions for slow and rapid rotators reported by Britavskiy et al. (2019).

[c]The observed clusters are IC 1805, IC 1848, NGC 6231, NGC 6611, Tr 16 and IC 2944.

[d]Studies taking into account both SB1 and SB2 bias for the intrinsic binary fraction.

instruments and technical setups, and their sensitivity to detect RV shifts thus varies. Furthermore, there is a selection bias toward binary systems with similarly bright components rather than single stars at the faint end of magnitude-limited samples (Vanbeveren & Conti 1980). To obtain the true, intrinsic binary fraction, the observed fractions have to be bias-corrected using the probability of detecting binary systems with a given observing campaign. This not only requires an assumption about the underlying orbital parameter distributions but also detailed knowledge of potential biases of the observing campaign (see, e.g., Sana et al. 2012). Comparing the intrinsic binary fractions (where available; see **Table 1**) demonstrates that a vast majority of massive stars are members of close binary systems. Despite large error bars, there seems to be a trend between binary fraction and stellar mass. Whether this is indeed related to the mass or potentially also to the metallicity or the age of the cluster remains to be constrained by further work.

Most surveys mentioned in **Table 1** consider only the so-called SB1 bias (the chance to detect RV shifts of a given binary system larger than a given detection threshold, often chosen to be 20 km s^{-1}). An additional bias, the so-called SB2 bias, arises from unidentified SB2 systems that appear as rapidly rotating single stars if their RV shifts are too small for their spectral lines to effectively deblend (see Sana et al. 2011, Bodensteiner et al. 2021). This effect becomes more important for stars that rotate more rapidly and for smaller RV variations, as well as for lower spectral-resolution data. In particular, it hampers the detection of equal-mass binaries, especially if they are in long period systems. Taking this bias into account will further increase some of the intrinsic binary fractions reported in **Table 1**.

Although some of the surveys mentioned in **Table 1** are based on a few epochs only (enough to measure RV variations and detect binaries), others had enough observations (i.e., $\gtrsim$20 epochs) to fit binary orbits and constrain orbital parameters for SB1s and SB2s. Furthermore, additional observing campaigns were designed to follow up on previously detected binary systems, for example, the MONOS (Multiplicity Of Northern O-type Spectroscopic systems) survey for Galactic O-star binaries (Maíz Apellániz et al. 2019, Trigueros Páez et al. 2021) or the TMBM (Tarantula Massive Binary Monitoring; Almeida et al. 2017) and BBC (B-type Binaries Characterisation; Villaseñor et al. 2021) programs that followed O- and B-type binaries from the VFTS, respectively.

The exponent of the period distribution, which is defined as $f(\log P[\text{days}]) \sim (\log P)^{\pi}$, is reported to vary between $\pi = -0.45 \pm 0.39$ for the Milky Way O stars (Sana et al. 2012) and $\pi \sim -0.2$ for the LMC O stars (Almeida et al. 2017), which is close to flat on $\log P$ (see, e.g., Banyard et al. 2022). The eccentricity distribution follows $f(e) \sim e^{\eta}$ with $\eta = -0.4 \pm 0.2$ (Sana et al. 2012). Covering a large range of mass ratios, Shenar et al. (2022a) reported that the mass-ratio distribution of VFTS binaries is also consistent with a flat distribution; that is, $f(q) \sim q^{\kappa}$ with $\kappa = -0.2 \pm 0.2$. Comparing the observed orbital parameter distributions derived from detected binaries in different spectroscopic works implies them to be universal across metallicity and the considered stellar mass range (for a compilation, see Banyard et al. 2022, their figures 8 and 10). The orbital properties of close, eclipsing binaries in the Milky Way, LMC, and SMC further corroborate that there are no statistically significant trends with metallicity (Moe & Di Stefano 2013).

Observations unambiguously show that a large majority of OB MS stars are in binary systems. Although the binary fraction seems to increase with stellar mass also outside the mass range considered here (for an overview, see, e.g., Moe & Di Stefano 2017), the uncertainties are still large. The orbital parameter distributions seems universal across mass and metallicity (down to the metallicity of the LMC), but more observations are required to further test this. The measured binary properties in young populations are thought to reflect the initial conditions, but their link to the outcome of star formation is not well understood (Duchêne & Kraus 2013). Early processes such as inward migration or binary hardening seem to also play a role (e.g., Sana et al. 2017, Ramírez-Tannus et al. 2021, Bordier et al. 2022). The picture is further complicated by the detection of triple or higher-order multiples (e.g., Lanthermann et al. 2023) and by postinteraction products polluting older populations and field stars (e.g., Wang et al. 2020).

3.2. OBe Stars

OBe stars are on average cooler and redder than their OB counterparts because of their rapid rotation and the IR excess from the disk (for a recent review, see Rivinius et al. 2013). Different channels explaining the rapid rotation of OBe stars have been proposed. Those include their interpretation as single stars that approach critical rotation toward the end of the MS (e.g., Granada et al. 2013, Hastings et al. 2020b) or as mass gainers in previous binary interactions (e.g., Pols et al. 1991, Hastings et al. 2021). A potential way to distinguish those is to constrain OBe multiplicity properties: According to the single-star channel, OBe stars should have similar binary properties as OB stars. According to the binary channel, there should be a lack of MS companions and a significant number of stripped companions or compact objects. However, large-scale surveys constraining close binary properties of entire samples of classical OBe stars are mostly lacking, in particular in comparison to works on OB stars (Section 3.1). Additionally, OBe spectra exhibit variability both in their disk emission and through stellar pulsations (e.g., Barnsley & Steele 2013, Baade et al. 2016, Labadie-Bartz et al. 2022), complicating binary detections.

Classical OBe: rapidly rotating, nonradially pulsating late-O- and B-type stars whose spectra show, or have shown, emission lines that are formed in a gaseous circumstellar decretion disk

Red supergiants: evolved massive stars; they often mark the final stage of evolution before ending their lives with a supernova explosion

Abt & Levy (1978) studied a small sample of B and Be stars, reporting similar binary properties; however, their findings were based on low-quality data. High angular resolution imaging and speckle interferometry studies reported a similar result, but their observations are not sensitive to short periods relevant for binary interactions (Oudmaijer & Parr 2010, Horch et al. 2020). Although Klement et al. (2019) interpreted a detected turn-down in the spectral energy distributions of OBe stars as indicative of the presence of a companion truncating the disk, their nature remains unconstrained. Using multiepoch observations of the young SMC cluster NGC 330, Bodensteiner et al. (2021) reported a significantly lower binary fraction of Be stars compared to B-type stars in the same cluster.

Concerning Be star companions, Bodensteiner et al. (2020c) pointed out a lack of close MS companions to massive Be stars based on a literature study.[3] These should be the easiest to detect and are the most common companions to OB stars (Shenar et al. 2022a). In contrast, the sample of Be binaries with bloated stripped stars and subdwarf OB (sdOB) companions is continuously increasing (e.g., Wang et al. 2021, El-Badry & Quataert 2021; see Section 5.2). A well-studied class of Be binaries are Be X-ray binaries (BeXRBs) that are detected based on their X-ray emission (e.g., Raguzova & Popov 2005, Reig 2011, Coe & Kirk 2015; see also Section 6.1).

Overall, the binary properties of OBe stars remain fairly unconstrained and the orbital parameters distributions cannot be constructed from the few available measurements. The overall binary fraction of OBe stars seems to be lower than that for OB stars, whereas the companions are predominantly stripped stars or compact objects. This is in line with expectations of the binary channels of Be star formation, but further observations are required to consolidate or falsify this. On the lower-mass end (for late-type Be stars), the single-star channel might play a more important role (e.g., Kervella et al. 2008, Klement et al. 2021).

3.3. Red Supergiants

Given the difficulty in observationally distinguishing between red supergiants (RSGs) and low-mass stars in the Milky Way (Healy et al. 2023), the number of known RSGs in our Galaxy is low. Because of their large radii of up to 1,500 $R_\odot$, short-period binaries interact before the RSG phase, resulting in a lack of RSGs in close binaries (in contrast to their OB progenitors). On one hand, this implies that many RSGs could be the rejuvenated products of previous interactions (dubbed red stragglers; Britavskiy et al. 2019). On the other hand, it means that surviving RSG binaries have long orbital periods, which in combination with their intrinsic RV variability (e.g., Josselin & Plez 2007) hampers binary detections and could hide potential signatures of companions.

Only a few binarity estimates exist for Galactic RSGs. One of those was conducted by Burki & Mayor (1983), who detected 19 binaries among 181 northern RSGs with optical spectroscopy and,

[3]A possible exception is δ Scorpii, which was reported to be in a long-period, highly eccentric binary system with a MS companion but also to be a runaway triple system with another, yet undetected companion (e.g., Tango et al. 2009, Meilland et al. 2011).

combined with previously known RSG binaries, reported a binary fraction of ∼20%. Most multiplicity studies target RSGs in our neighboring galaxies. Compiling archival RV measurements of almost 1,000 candidate RSGs in the LMC and SMC, Dorda & Patrick (2021) find a minimum binary fraction of $15 \pm 3\%$. RSGs with OB companions can be detected based on signatures in the blue part of the spectrum (Neugent et al. 2018). Using this method and spectroscopic follow-up observations, Neugent et al. (2019) measured a bias-corrected binary fraction of $20 \pm 7\%$ for RSGs in the LMC. Patrick et al. (2019) investigated multiepoch spectroscopy of 17 candidate RSGs in the 30 Dor region in the LMC observed in the context of the VFTS survey. Given that the detection probability for systems with periods up to 10,000 days and mass ratios >0.3 is estimated to be almost 90%, the observed and intrinsic binary fractions are similar, namely ∼30%. Patrick et al. (2020) further investigated the binary properties of 15 RSGs in the 35–40-Myr-old SMC clusters NGC 330 with multiepoch spectroscopy. They report a bias-corrected binary fraction of $30 \pm 10\%$ for orbital periods between $2.3 < \log P(\text{days}) < 4.3$ and mass ratios >0.1.

Based on UV photometry, Patrick et al. (2022) measured an intrinsic binary fraction of $18.8 \pm 1.5\%$ for >500 RSGs in the SMC for mass ratios >0.3 and periods above 1,000 days. They find indications for a flat mass-ratio distribution and a lack of high mass-ratio ($q > 0.5$) systems above 15 $M_\odot$ (implying an absence of companions with similar masses to that of the RSG); thus, the authors interpreted the most massive RSGs as being merger products. Neugent (2021) extended the investigation to the Local Group galaxies M31 and M33. They reported a constant binary fraction of $33.5^{+8.6}_{-5.0}\%$ for M31, whereas the binary fraction in M33 drops from $41.2^{+12.0}_{-7.3}\%$ to $15.9^{+12.4}_{-1.9}\%$ for inner and outer regions, respectively, which is attributed to a metallicity effect.

Overall, the intrinsic binary fractions of RSGs measured in the SMC and LMC using different detection techniques are in agreement with each other and amount to ∼20% for $q > 0.3$. Interestingly, so far no RSGs with O-type companions are reported, but they should be more easily detectable than their B-type counterparts. The role of metallicity and the nature of the companions of those RSGs, as well as the orbital parameter distributions, remain to be further constrained.

Luminous blue variables: hot and highly variable stars located in the upper region of the HRD, which can be above the Humphreys–Davidson limit

Wolf–Rayet (WR) stars: spectral classification based on strong, broad emission lines; includes classical WRs (cWR) without hydrogen lines and nitrogen-rich WRs with hydrogen lines (WNh)

3.4. Luminous Blue Variables

Whereas luminous blue variables (LBV) were for a long time considered to be the transitory phase between single-star blue supergiants (BSGs) and Wolf–Rayet (WR) stars characterized by strong, eruptive mass loss (e.g., Conti 1975, Lamers & Nugis 2002), the link of LBVs as direct progenitors of type-II SNe induced a shift in their interpretation, not as a transitory phase but as a potential end point of stellar evolution (Kiewe et al. 2012, Groh et al. 2013). They were further proposed to be not a phase in single-star evolution but rather binary interaction products (see, e.g., Gallagher 1989, Justham et al. 2014, Smith & Tombleson 2015; see also Section 5). Constraining the binary properties of LBVs would thus also allow for putting constraints on their evolutionary history.

Given the rarity of LBVs and their strong (spectroscopic and photometric) variability (see, e.g., Humphreys & Davidson 1994), binary detections are difficult. Targeting individual objects with different methods, several binary LBVs have been found so far (see, e.g., Martayan et al. 2012, Boffin et al. 2016), but only a few systematic studies of the binary properties of LBVs exist. Based on an X-ray survey using XMM-Newton (*X-ray Multi-Mirror Mission–Newton*; Nazé et al. 2012) report X-ray properties for LBVs consistent with a binary fraction in the range of 26–69% (detecting signatures of wind–wind collisions and potentially the O-type companions themselves). Targeting seven LBVs with high angular resolution imaging, Martayan et al. (2016) find a binary fraction of ∼30%. Mahy et al. (2022a) combined spectroscopy and interferometry and reported a bias-corrected binary fraction for Galactic LBVs of $62^{+38}_{-24}\%$ for periods below 1,000 days and mass ratios between 0.1 and 1.0. The detected companions of LBVs are either OB MS stars or RSGs, and given the large radii of LBVs, the periods of those systems are large (e.g., Mahy et al. 2022a). The full orbital parameter distributions such as the period distribution remain largely unconstrained.

Blue supergiants (BGSs): stars of spectral type OB with luminosity class I

Yellow supergiants (YSGs): stars of spectral type OB with luminosity class I but cooler in temperature than BSGs

3.5. Wolf–Rayet Stars

Different types of stars fall under the spectroscopic definition of a WR star, which is based on strong, broad emission lines in the spectrum. Most WR stars are classical WR (cWR) stars, subdivided into nitrogen- (WN), carbon- (WC) or oxygen-rich (WO) depending on their surface composition. These are thought to be post-H-burning objects in an evolved stage of massive-star evolution after the RSG and potentially LBV phase. In contrast, most of the rare WNh stars (WN stars with hydrogen lines) are thought to be stars that are even more massive ($\gtrsim 100\,M_\odot$ at Galactic and LMC metallicity) on the MS with strong stellar winds (see, e.g., Crowther 2007, for a recent review). Conti (1975) proposed an evolutionary sequence between them: O/WNh → LBV → WN → WC (→ WO). If this connection exists, their binary properties should also align accordingly (i.e., the observed binary fraction should be the same or decrease in later stages as the stars evolve).

In general, and using a multitude of techniques, similar observed binary fractions of ∼30–40% were reported for the Milky Way (e.g., van der Hucht 2001; Dsilva et al. 2020, 2022, 2023), lower-metallicity (such as the LMC and SMC) (e.g., Foellmi et al. 2003a,b; Schnurr et al. 2008; and references therein), and higher-metallicity host galaxies (like the Triangulum or the Andromeda Galaxy; Neugent & Massey 2014). A study of stars of spectral type WNLha in the Arches cluster was reported to have a lower limit on the observed binary fraction of $\gtrsim$62% (Clark et al. 2023). High-resolution spectroscopy of Galactic WN and WC stars seem to indicate that the bias-corrected binary fraction of WN stars is lower (52^{+14}_{-12}%) than that for WC stars (96^{+4}_{-22}%) and that their period distributions differ (with a large number of short-period WN binaries; Dsilva et al. 2023, and references therein). Although Conti's evolutionary connection might hold for long-period systems, these short-period WN systems remain unexplained. Binary properties of WNh stars are largely unconstrained.

3.6. Blue and Yellow Supergiants

The class of BSGs (with luminosity class I) comprises several types of objects. O supergiants are massive stars toward the end of their MS evolution. B supergiants are interpreted as being in a transitory post-MS phase, in either a brief traverse over the HRD or during a blue loop (Maeder & Meynet 2001, Vink 2022). Long-lived BSGs were suggested to be the product of stellar mergers. One particular case is that of SN1987A, which occurred in the LMC. Pre-explosion images indicated its progenitor was a BSG, which can be naturally explained as a merger product (Podsiadlowski et al. 1990, Menon & Heger 2017). Yellow supergiants (YSGs) are a heterogeneous group of stars crossing the HRD (Maeder & Meynet 2000). Stars even more luminous than these are referred to as hypergiants (with luminosity class I+ (de Jager 1998).

The binary properties of BSGs and YSGs are not well constrained. In the context of the VFTS, Dunstall et al. (2015) reported an observed binary fraction of B-type supergiants of 23 ± 6%, in agreement with that observed for MS B-type stars targeted in the same survey. Observing OB giants to supergiants in the Galactic clusters Westerlund 1 with VLT-FLAMES, Ritchie et al. (2022) found an observed binary fraction of $\gtrsim$40%, noting that the intrinsic fraction might be significantly larger. Clark et al. (2023) reported a lower limit of 29% on the observed binary fraction of O-type hypergiants in the Arches cluster.

4. BINARY INTERACTION PROCESSES

To constrain the role of binary interactions in the observed properties of systems described in Section 3, we discuss the main processes that alter the evolution of stars in binary systems. We first cover how interactions and long-term evolution are currently simulated.

Rapid binary code: based on fits to single-star models and semianalytical approximations to binary interactions; has run times smaller than a CPU second

Detailed binary code: 1D code that solves the differential equations of stellar structure and evolution for a binary; has run time on the order of a CPU hour

4.1. Modeling Tools for Binary Evolution

Following the evolution of a binary system, including the properties of both its components requires the use of computer simulations. Three different types of codes are used for this purpose. Multidimensional (magneto-)hydrodynamical simulations can be used to probe short dynamical timescales, which is useful to model processes such as mergers and CE evolution (e.g., Lombardi et al. 1995, Taam & Sandquist 2000, Schneider et al. 2019, Lau et al. 2022). In 3D codes, various simulation approaches are used, including smoothed particle hydrodynamics as in `GADGET` (Springel et al. 2001) and `StarSmasher` (Gaburov et al. 2010), grid-based calculations with adaptive mesh refinement as in `FLASH` (Fryxell et al. 2000) and `ATHENA++` (Stone et al. 2020), and moving-mesh simulations as in `AREPO` (Springel 2010). Due to their computational cost, 3D simulations can only explore a limited set of initial conditions and cannot resolve nuclear and thermal timescale mass-transfer processes. To model longer evolutionary timescales, 1D stellar evolution codes are used, which at their core carry a significant resemblance to the models computed over half a century ago by Kippenhahn & Weigert (1967). 1D stellar evolution codes also serve as the source for initial conditions of 3D simulations. The third type of simulations are referred to as rapid codes or rapid binary codes and are based on semianalytical models based on precomputed 1D stellar models (e.g., Hurley et al. 2002) that allow for subsecond calculation of full binary evolution models.

In contrast to rapid codes, 1D simulations are referred to as “detailed.” The majority of models currently computed with detailed binary codes are done with the `MESA` code (Paxton et al. 2011, 2015) or variations of the `STARS` code (Eggleton 1971, Eldridge et al. 2008), but important work in the past decade has also been carried out with the `BEC` code (see Yoon et al. 2010, and references therein). These codes are derived from the Henyey method (Henyey et al. 1959) to solve the equations of stellar structure in 1D, computing the evolution of two stars that are coupled through tidal interaction (see Section 4.2) and mass transfer (see Section 4.3). Detailed models can accurately follow phases of evolution on the nuclear and thermal timescales of its components, including phases of contact (see Section 4.4). Using 1D codes to model dynamical phases of evolution requires approximations that ignore (or parameterize) the uncertainties associated with 3D binary interactions (see Section 4.5).

Compared to detailed evolutionary codes, a much broader set of tools are available to perform rapid calculations. A majority of these are based on the analytical fits of Hurley et al. (2000) to the single-star evolutionary models of Pols et al. (1998), coupled with the semianalytical approximations to binary evolution of Hurley et al. (2002). These include `Startrack` (Belczynski et al. 2002), `binary_c` (Izzard et al. 2004), `MOBSE` (Giacobbo & Mapelli 2018), `COSMIC` (Breivik et al. 2020), and `COMPAS` (Riley et al. 2022). Even though these codes include multiple free parameters to adjust the physics of binary evolution, they are limited to the physical assumptions of the stellar models of Pols et al. (1998). Some examples that break from this reliance on the fits of Hurley et al. (2002) are `COMBINE` (Kruckow et al. 2018), `METISSE` (Agrawal et al. 2020), and `SEVN` (Iorio et al. 2023). Additionally, various codes precede the work of Hurley et al. (2002), including `SeBa` (Portegies Zwart & Verbunt 1996), and the Brussels population-synthesis code (Vanbeveren et al. 1998). One main weakness of rapid evolutionary codes is that, because they are based on single-star evolutionary models, they cannot capture the response of thermal timescale mass transfer on either component, which plays a critical role in determining the stability of mass transfer.

Owing to their short runtimes, rapid codes have been the preferred tool to perform population synthesis calculations (see Han et al. 2020 for an overview), but detailed calculations are continuously taking a larger role in this area. Large grids of detailed models have been usually restricted to limited regions of the input parameters [e.g., the grids of Case A evolution of Nelson & Eggleton (2001), de Mink et al. (2007), and Sen et al. (2022)]. Currently, the `BPASS` (Eldridge et al. 2017) and `POSYDON` (Fragos et al. 2023) codes (which use `STARS` and `MESA` as their backends, respectively) provide openly available sets of detailed calculations covering the full range of parameters relevant to interacting massive binaries. Other large-scale population synthesis calculations done with detailed models have been performed (e.g., Wang et al. 2020) but do not have an associated name. Although detailed population synthesis calculations are now feasible, further increasing the efficiency of calculations is critical for reproducibility and broad testing of theoretical uncertainties. One approach is the use of smart sampling of initial parameters rather than the use of a regular grid, coupled with interpolation (Rocha et al. 2022).

4.2. Tidal Interaction

Tidal torques in stars with radiative envelopes are attributed to the dynamical tide process (Zahn 1975; see Zahn 2008 for a recent review). In this process, gravity modes are excited by the tidal potential near the interface between the convective core and the radiative envelope, with these waves dissipating close to the stellar surface. The work of Zahn (1975) provides a straightforward method for computing the rate of tidal synchronization and circularization, with the only nontrivial dependency being the computation of the structure constant E_2. Many simulations (Hurley et al. 2002, Paxton et al. 2015) relied on an interpolation to the values of E_2 for zero-age MS models computed by Zahn (1975), but more modern calculations accounting for evolved stages are available (Qin et al. 2018). Extensions to the Zahn (1975) model have also shown the potential for resonant interactions when the tidal frequency matches a natural oscillation frequency of the star, potentially leading to resonance locking (Witte & Savonije 1999). Direct calculations of the tidal torques are now possible on a timescale that allows for their integration in evolutionary calculations (e.g., Sun et al. 2023). Computations of this type, relaxing some of the assumptions made by Zahn (1975), have shown that in some cases tidal interaction arises from standing waves rather than traveling waves that are completely damped at the surface (Ma & Fuller 2023).

An associated growing field of study is the observation and theory of tidally excited oscillations in eccentric binaries (e.g., Fuller 2017, Guo 2021, and references within). The discovery of the prototypical system KOI-54 (Welsh et al. 2011) was enabled by the short cadence and high precision observations of the *Kepler* telescope. Owing to their characteristic light curves, such systems are often referred to as heartbeat stars. The two components of KOI-54 are only about twice the mass of the Sun, but despite not being massive they allow researchers to probe tidal processes in stars with radiative envelopes. Further observations have pushed the observed heartbeat systems to the massive star regime, with TESS observations showing a system with a total mass of $\sim 150\,M_\odot$ (Kołaczek-Szymański et al. 2021).

One aspect that has received less attention is the effect of tidal deformation. Although tidally deformed stellar surfaces following the Roche potential are used to model observations (e.g., Prša & Zwitter 2005, Abdul-Masih et al. 2020), the impact of deformation on interior structure is seldom included in evolutionary models. By extending methods used to model centrifugal deformation in 1D stellar models, Fabry et al. (2022) has incorporated tidal deformation in binary evolution models, which can be applied to detached, semidetached, and contact binary systems.

Another approach by Fellay & Dupret (2023) accounts for the full nonspherical mass distribution of each component in order to construct static structure models. Extended studies describing how tidal deformation modifies binary evolution are not available at the moment.

4.3. Stable Mass Transfer

When a star in a binary fills its Roche lobe, mass transfer ensues and modifies both the orbit and the structure of the donor. Whether or not the donor can remain in hydrostatic equilibrium in these conditions is normally described in terms of the mass radius exponents,

$$\zeta_{\rm ad} \equiv \left(\frac{d\log R}{d\log M}\right)_{\rm ad}, \quad \zeta_{\rm RL} \equiv \frac{d\log R_{\rm RL}}{\log M}, \qquad 5.$$

which describe the adiabatic response of the donor radius and the change in the Roche lobe radius as mass is transferred (e.g., Soberman et al. 1997). If $\zeta_{\rm ad} > \zeta_{\rm RL}$, the donor can adjust to mass transfer while remaining in hydrostatic equilibrium, producing either nuclear or thermal timescale events. In particular, donor stars with a significant fraction of their mass in a convective envelope are expected to expand in response to mass loss (Hjellming & Webbink 1987), favoring instability for late Case B and Case C mass transfer (see **Figure 1**). In detailed evolutionary calculations, this criteria is less useful, as $\zeta_{\rm ad}$ cannot directly be inferred from the structure of the star. In certain cases, the pressure scale height at the photosphere can be an important fraction of the stellar radius, making the concept of a hard surface limited by its Roche lobe inapplicable. Such conditions require a different method to evaluate instability (Temmink et al. 2023). Rapid evolutionary codes rely on prescribed stability criteria, leading to significant uncertainties in the predicted rates and formation processes of merging binary black holes (BHs) (Gallegos-Garcia et al. 2021, Olejak et al. 2021).

Figure 3 shows the typical evolution of two binaries undergoing stable Case A and early Case B mass transfer, which closely resembles the evolution of the donor stars of Kippenhahn & Weigert (1967). Unless the evolution is modified by the secondary filling of its own Roche lobe, Case A mass transfer is expected to be separated into a "fast" and a "slow" phase. As the more massive star in the Case A system initiates mass transfer, the orbit shrinks and leads to a thermal timescale mass transfer event. After the mass ratio inverts and the donor can thermally relax into the size of its Roche lobe, mass transfer is driven by nuclear evolution. This evolutionary stage is referred to as the Algol phase, and owing to the large ratio between thermal and nuclear timescales, a large majority of observable semidetached systems are expected to be in this phase (e.g., Mahy et al. 2020). After the MS, a final phase of Case AB mass transfer strips most of the remaining envelope and leaves a star mostly composed of helium. The Case B system instead interacts, whereas its expansion is driven by hydrogen shell burning and results in a single fast phase of Case B mass transfer removing most of the hydrogen envelope.

Various processes can modify this classical picture of the evolution of massive binary stars. Rapid rotation is argued to produce chemically homogeneous evolution in massive stars (Maeder 1987), in which case the MS evolution proceeds at an almost constant radius. de Mink et al. (2009) argued that for massive binaries born near contact, tidal synchronization leads to rapid rotation and chemically homogeneous evolution of the primary, resulting in the first mass transfer phase being initiated by the initially less massive star (see also Marchant et al. 2017). Regarding the Algol phase, Sen et al. (2023) showed that as more massive stars have a larger fraction of their mass in their convective cores, for sufficiently high donor masses ($\gtrsim 30\,M_\odot$) the helium-enriched core can be exposed before the mass ratio inverts. If that happens, the star can thermally relax to its Roche lobe size before mass ratio inversion, leading to a slow Case A phase with a more massive donor

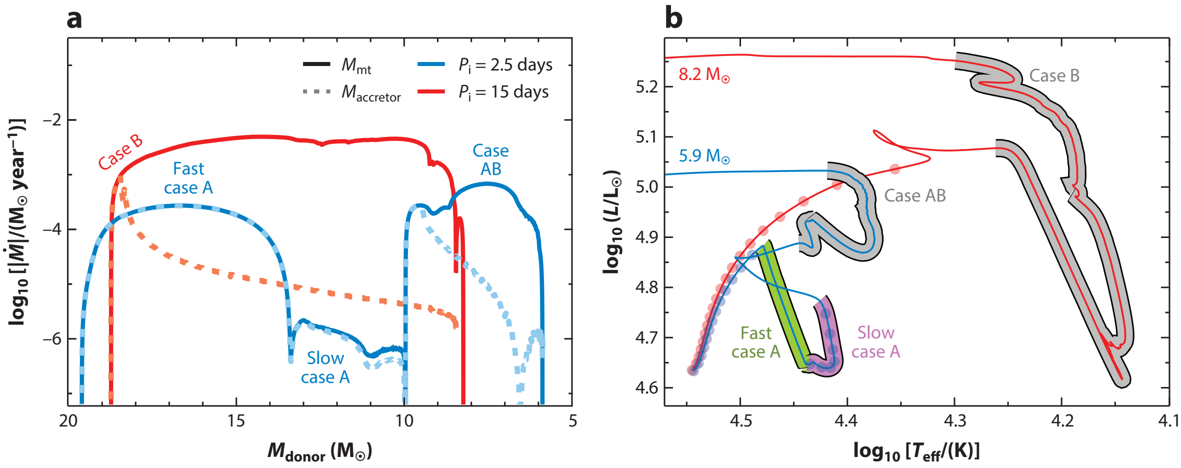

Figure 3

(*a*) Mass transfer rate $\dot{M}_{\rm mt}$ and rate of change of mass of the accreting star $\dot{M}_2$ as a function of the donor mass for a case A system ($20\,M_\odot + 16\,M_\odot$ with an initial period of 2.5 days) and an early Case B system (same masses but with an orbital period of 15 days). Simulations include rotation, and mass accretion is limited after the accreting star reaches critical rotation. (*b*) Evolution of the donor star in the HRD for the same two binaries. Different mass transfer phases are indicated with thick contours, and dots are placed in time intervals equal to 5% of the main sequence lifetime of the donor star. Masses of the resulting stripped stars are indicated. Abbreviation: HRD, Hertzsprung–Russell diagram.

than accretor (which Sen et al. 2023 refer to as reverse Algol). Regarding Case B mass transfer, Klencki et al. (2022) has suggested that at metallicities smaller or equal to that of the LMC, the thermal mass transfer phase can be interrupted and followed by a long-lived nuclear timescale phase with BSG or YSG donors.

Mass accretion onto the secondary results in increased rotational velocities and contamination with CNO processed material from the donor. These are seen as key indicators of past interactions, but are unfortunately degenerate with expectations of rotational mixing. As postinteraction secondaries can become overluminous and evolve to long periods (or become single stars in case the primary undergoes a SN), apparently single stars can actually be predominantly postinteraction products (de Mink et al. 2014). Our theoretical understanding of CNO enrichment and spin-up through accretion has not evolved significantly in the past decade, and the reader is referred to sections 3.1 and 3.2 of Langer (2012).

One critical aspect that remains unsolved is the interplay between mass transfer efficiency (i.e., how much of the mass transferred by the donor is accreted onto the companion) and accretion spin-up. As shown by Packet (1981), an accreting star needs only to increase its mass by a few percent before reaching critical rotation. Whether or not accretion can proceed from that stage is uncertain. Langer et al. (2003) has pointed out that in the shortest period systems, tidal interactions can prevent the accretor from reaching critical rotation, allowing for further accretion (see also Sen et al. 2023). It has also been argued that angular momentum could be transported outward from the accretion disk while still allowing for an inward mass flow (Paczynski 1991, Popham & Narayan 1991). Observational constraints are usually restricted to either the postinteraction or the Algol phase, whereas nonconservative phases are likely associated with thermal timescale mass transfer. Algol systems in the SMC appear to support a lowered efficiency with initial orbital period (de Mink et al. 2007), but other postinteraction systems favor high accretion efficiencies even at long orbital periods (e.g., Schootemeijer et al. 2018, Bodensteiner et al. 2020b, Vinciguerra

Mass transfer efficiency: fraction of mass transferred, which is added to the accretor; remainder mass can form a circumbinary disk or be ejected et al. 2020). A keystone system to understand accretion efficiency is the massive binary β Lyrae (e.g., Mourard et al. 2018), which is currently undergoing a rapid mass-transfer phase and has been resolved with the CHARA (Center for High Angular Resolution Astronomy) interferometer.

Another limitation of detailed binary models is that mass transfer rates are computed from prescriptions that use the 1D structure of the donor. A commonly used prescription is that of Kolb & Ritter (1990), which treats separately the contributions from the extended atmosphere of the donor stars as well as from regions below the photosphere that are above the L1 equipotential. Lightening the assumptions of the Kolb & Ritter (1990) model (Marchant et al. 2021) or taking a different approach altogether to the computation of mass transfer rates (Cehula & Pejcha 2023) leads to qualitatively different evolution during fast mass transfer phases, with the potential to undergo overflow of the outer Lagrangian points.

4.4. Contact Binaries

Contact binaries, where both components extend beyond the L1 equipotential, are precursors to stellar mergers and represent the most compact binary configurations possible. So long as material is contained within the equipotential of the second Lagrangian point L2, hydrostatic equilibrium is possible (Kuiper 1941). Just as with rotating stars, hydrostatic equilibrium in radiative layers requires the radiative flux to be proportional to gravity (e.g., Fabry et al. 2022). However, the von Zeipel paradox (von Zeipel 1924) does not allow for both radiative and thermal equilibrium to hold simultaneously, such that large-scale flows arise (Smith & Smith 1981, Tassoul & Tassoul 1982) and the surface flux deviates from a simple proportionality to effective gravity (e.g., Espinosa Lara & Rieutord 2012). Contact binaries are expected to have similar temperatures at their surfaces, implying that the luminosity ratio between the two components is similar to the mass ratio ($L_1/L_2 \simeq m_1/m_2$; Lucy 1968). Owing to the steepness of the mass–luminosity relationship, a significant redistribution of the luminosity beyond the L1 equipotential is needed.

The internal structure of massive contact binaries, including tidal deformation and energy transport, is not well understood, with early work from the 1970s not reaching a consensus (see Shu et al. 1980, and references within). Evolutionary models have characterized the conditions under which contact evolution happens, including the expansion of the accretor during thermal timescale mass transfer as well as the case in which the more massive secondary in an Algol system expands due to nuclear evolution (Eggleton 1996, Nelson & Eggleton 2001, Wellstein et al. 2001). Modeling the evolution after that stage has remained uncertain, with models that either ignore the different physics of the contact stage or use an ad hoc mass transfer rate determined such that the surface of both stars remains in the same equipotential (de Mink et al. 2007, Marchant et al. 2016). Population synthesis calculations of the LMC using this mass-transfer model indicate an overestimation of massive contact systems with mass ratios $\simeq$1 when compared with observations (Menon et al. 2021), as most contact systems with mass ratios away from unity are predicted to evolve in a thermal timescale toward equalization of masses. Initial calculations by Fabry et al. (2022, 2023) show that the inclusion of energy transport in evolutionary models of massive contact binaries can extend long-lived phases of evolution with mass ratios away from unity.

As the components of a short period contact binary rotate rapidly, rotational mixing is expected to make them overluminous and rich in nitrogen at their surface (and potentially operate more efficiently than in single-star evolution; Hastings et al. 2020a). Observations of the contact binary VFTS 352 (Almeida et al. 2015), containing a $\sim$30 $M_\odot$ + 30 $M_\odot$ binary with a period of 1.1 days, showed the system was indeed overluminous, providing potential support for rotational mixing and chemically homogeneous evolution. However, through detailed spectroscopic analysis accounting for the variable effective temperature across the surface, Abdul-Masih et al.

(2019, 2021) did not find an indication of enrichment with CNO processed material. Whether or not rotational mixing is active in massive contact stars remains an open question. The systems analyzed by Abdul-Masih et al. (2019, 2021) show that both components share similar effective temperatures and luminosities, which is consistent with the scenario in which energy is efficiently transferred across the shared layers. Abdul-Masih et al. (2022) also showed that for a selection of contact binaries with data spanning more than a decade, the evolution of their orbital periods could be constrained to operate on their nuclear timescales, independent of their mass ratios.

4.5. Mergers and Common Envelope Evolution

As a contact binary grows beyond its L2 equipotential, outflows removing large amounts of angular momentum are expected to lead to a quick coalescence (e.g., Pejcha et al. 2016). Stellar mergers can naturally be confused with single stars, but current binaries could also be the result of a merger in triple systems as suggested for η Carinae (Hirai et al. 2021), HD 45166 (known as a quasi-WR star; Shenar et al. 2023), and even higher multiplicity systems (Vigna-Gómez et al. 2022). It has been argued that the origin of magnetic stars is associated with amplification processes during a stellar merger (Ferrario et al. 2009). Magnetohydrodynamical merger simulations by Schneider et al. (2019) showed that sufficiently strong fields are produced, and they identified the magnetorotational and Kelvin–Helmholtz instabilities as amplification processes. However, even if sufficiently strong magnetic fields are produced, they could be short lived. Strong magnetic fields introduce an additional timescale associated with Alfvén waves traveling through the star, and there are significant restrictions on the geometry of the field for it to be stable on this timescale (Braithwaite & Spruit 2004).

A merger can also be the outcome of unstable mass transfer leading to CE evolution. Whether or not a binary undergoing CE survives (ejecting its shared envelope) or merges is a long-standing problem (see Ivanova et al. 2013 and Röpke & De Marco 2023 for recent reviews). Being one of the main formation channels proposed for binary neutron stars (NSs; e.g., Tauris et al. 2017, Vigna-Gómez et al. 2018) and merging binary BHs (e.g., Belczynski et al. 2016, Bavera et al. 2021), uncertainties in CE evolution lead to order-of-magnitude uncertainties on compact object merger rates (Mandel & Broekgaarden 2022).

As individual CE simulations of massive stars are expensive (e.g., Lau et al. 2022, Moreno et al. 2022), population predictions are reliant on simplified approximations. The most common approach is the use of the energy balance criterion, in which the change in orbital separation is computed in terms of the binding energy of the envelope of the star initiating the CE phase and a free efficiency parameter (Webbink 1984). Rapid population synthesis codes make use of fits to precomputed binding energies as a function of the evolutionary stage of the star, but it has been recently pointed out that these could severely underestimate binding energies and overpredict the amount of stars surviving CE evolution (Klencki et al. 2021, Marchant et al. 2021). The computation of binding energies is also very uncertain, as it is not known a priori how much mass will be ejected before the CE. Recent results indicate that post-CE, the donor does not necessarily contract to become a hot stripped star but rather undergoes a phase of stable mass transfer that completes the envelope stripping process (Fragos et al. 2019, Marchant et al. 2021, Hirai & Mandel 2022).

5. NONDEGENERATE POSTINTERACTION PRODUCTS

Binary interactions, which are predicted to occur in a large number of stars in close binaries, drastically change the evolution of the system. This implies that a large number of postinteraction products should exist (e.g., de Mink et al. 2014, Schneider et al. 2015, Britavskiy et al. 2019,

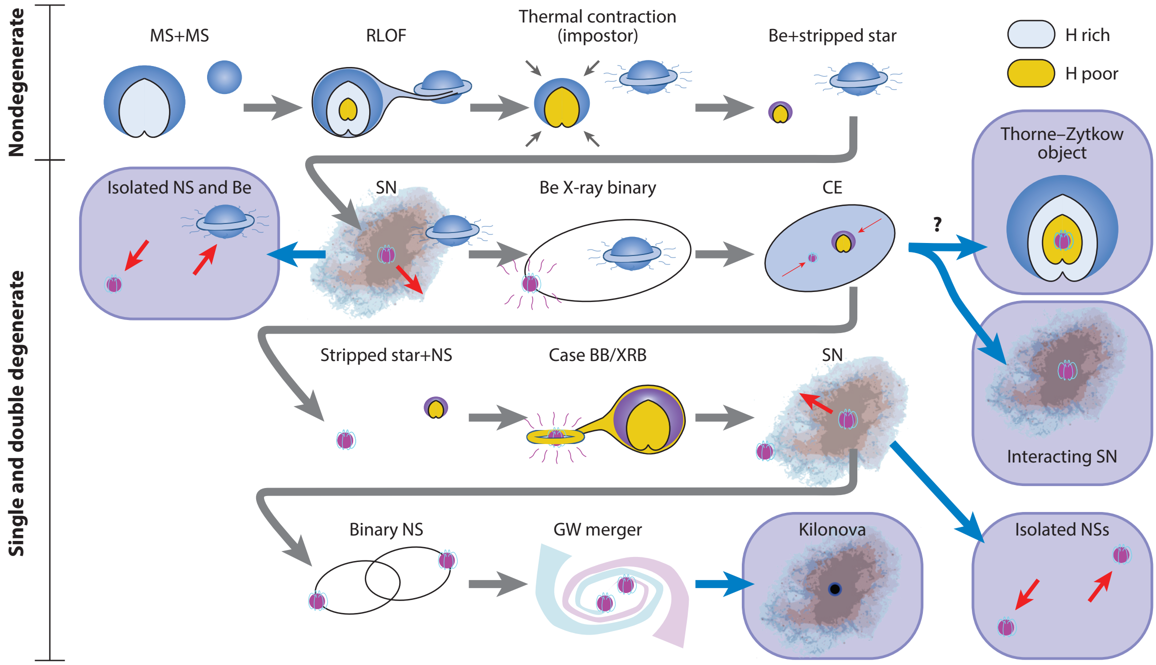

Figure 4

Evolution of a massive binary from birth until the formation of a GW source, showing various intermediate postinteraction products. Blue boxes represent end points for binary evolution. Abbreviations: CE, common envelope; GW, gravitational wave; MS, main sequence; NS, neutron star; RLOF, Roche lobe overflow; SN, supernova; XRB, X-ray binary.

Wang et al. 2020). The different evolutionary channels described in Section 4 can lead to a multitude of interaction products with different properties, depending on the type of interaction. Whereas several characteristics were proposed to identify interaction products (see, e.g., de Mink et al. 2014, for a list of observational indications), none of them are unambiguous. This implies that many undetected interaction products might be interpreted as single or noninteracting stars. As pointed out by de Mink et al. (2014), the best single stars are most likely stars in preinteraction binaries, which are usually detected via RV variations (Section 3.1).

Postinteraction binaries offer fundamental tests of evolutionary models, which need to reproduce not only the numbers but also the properties of key postinteraction systems like He-star binaries, WR binaries, OB stars with compact companions, HMXBs, and many more (see **Figure 4**). Including interaction products in our understanding of stellar populations is crucial. For example, binary interactions were proposed to be responsible for the split MSs observed in young star clusters (Milone et al. 2018; Wang et al. 2020, 2022). Furthermore, stars that have undergone binary stripping during their evolution are predicted to significantly impact the integrated spectrum of stellar populations (Götberg et al. 2019) and change their ionizing budget (Götberg et al. 2020). Stripped stars are further thought to produce systematically different SN yields (Laplace et al. 2021; Farmer et al. 2021, 2023a).

An example of the evolution of a massive binary is schematically depicted in **Figure 4**. It demonstrates the multitude of different intermediate stages of interaction products, both nondegenerate (described here) and single or double degenerate (described in Section 6) with different observational characteristics. It also illustrates potential end points of binary evolution, which depend on the parameters of the system and the type of interaction that occurs. **Figure 5** shows

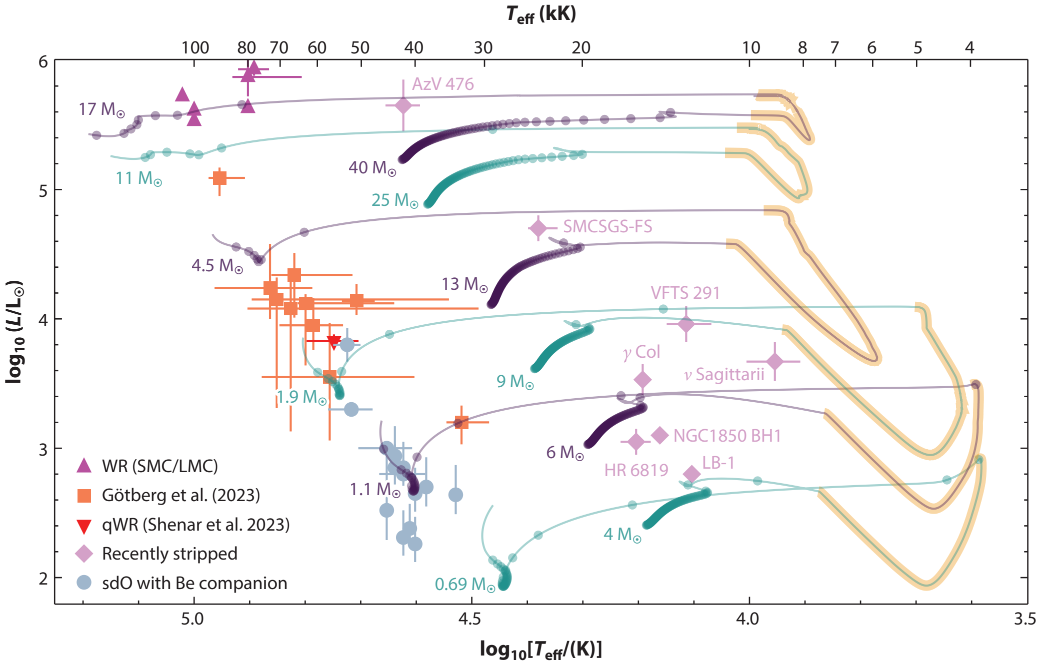

Figure 5

Observational sample of binary-stripped stars. The HRD shows the relation between bloated, recently stripped stars (*light pink diamonds*) and their contracted successors. It further shows that the mass gap between sdO stars (*gray circles*) and WR stars (*pink triangles*) was recently filled with intermediate-mass stripped stars (*orange squares*). Evolutionary tracks for donor stars of different masses undergoing case B mass transfer are shown, indicating their zero-age MS mass as well as their mass after stripping. Dots in the tracks are placed at intervals equal to 1% of the MS lifetime, and thick orange lines indicate phases of mass transfer. Abbreviations: HRD, Hertzsprung–Russell diagram; LMC, Large Magellanic Cloud; MS, main sequence; sdO, subdwarf O; SMC, Small Magellanic Cloud; qWR, quasi-Wolf–Rayet; VFTS, VLT-FLAMES Tarantula Survey; WR, Wolf–Rayet.

an observational overview of the mass donors in different mass regimes and evolutionary stages postmass transfer in an HRD. We here include (candidate) objects detected by various techniques, which are described in the subsections below, and refrain from adding the mass gainers, as often their parameters are not well constrained.

5.1. Potential Merger Products

Merger products are important in different aspects. As described in Section 3, the BSG progenitor of SN1987A can be explained as a merger product in a binary context, but not with a single-star solution (e.g., Podsiadlowski et al. 1990, Menon & Heger 2017). Blue straggler stars, which are located above the MS turnoff in clusters, could be rejuvenated merger products (e.g., Sills et al. 2002), which shape the mass function of entire stellar populations (Schneider et al. 2015). Wang et al. (2022) proposed the blue component of the split MSs observed in young star clusters to be formed by pre-MS mergers.

A handful of massive stars are potential stellar merger products. Betelgeuse was recently proposed to be the product of a stellar merger that occurred hundreds to thousands of years ago (e.g., Chatzopoulos et al. 2020). Another famous example is the prototypical LBV η Car, which is currently in an eccentric binary system. Its giant eruption in the nineteenth century was proposed to be produced by the merging of the inner binary in a previous triple system (Portegies Zwart

& van den Heuvel 2016, Smith et al. 2018, Hirai et al. 2021). Whether other LBVs could be the product of a stellar merger remains to be constrained. Mergers might also be one possible cause of the class of B[e] stars (for example, R4 in the SMC; Pasquali et al. 2000). Similar to R4, the potential merger HD 148937, a rapidly rotating, magnetic O6.5f?p star, is surrounded by bipolar, N-rich circumstellar nebula, which was attributed to mass ejected during the merger process (for a detailed discussion, see Langer 2012, Frost et al. 2021).

Another proposed merger product is the slowly rotating early B star τ Scorpii (spectral type B0.2V; Keszthelyi et al. 2021). Its spectrum shows a strong nitrogen excess (e.g., Martins et al. 2012), and the star is associated with a large-scale complex magnetic field (e.g., Petit et al. 2013). Schneider et al. (2019) reproduced the observed properties of τ Sco by a magnetohydrodynamic model of two merging MS stars, including its younger age in comparison to its parent association, the Upper Sco region. Similar age arguments were proposed for HR 2948 (it appears younger than a potential binary companion; Schneider et al. 2016) and, more recently, the Galactic runaway HD 93521 (it appears younger than the time it would have taken to travel from the Galactic disk to its current location; Gies et al. 2022). An additional merger candidate is ζ Puppis (Vanbeveren 2012). Interestingly, their rotational properties are quite different: Although HD 93521 and ζ Pup are rapid rotators, τ Sco is an extremely slowly rotating star (Nieva & Przybilla 2014).

Another proposed merger product is HD 45166, which was previously denoted quasi-WR due to its spectral appearance (it has similar, but narrower, emission lines than normal WR stars; see, e.g., Steiner & Oliveira 2005, and references therein). It was initially interpreted as a first example of an intermediate-mass stripped star bridging the mass gap between sdOBs and WRs (see Section 5.2) but was recently reported to exhibit a strong magnetic field of 43 kG. This makes it a potential progenitor of a magnetar, i.e., a highly magnetized NS. To explain its properties, a merger of a hydrogen-rich star with a stripped star was proposed that expelled most of the H-rich envelope (Shenar et al. 2023). Given the proposed involvement of a stripped star, we include it in **Figure 5**.

5.2. Observations of Stripped Stars

It was long proposed that to form cWRs, envelope stripping occurs because of either strong stellar winds (e.g., Crowther 2007) or mass transfer in binary systems (e.g., Paczyński 1967, Vanbeveren et al. 1998). The role of each channel remains uncertain, which may vary as a function of the metallicity in a nontrivial manner (Shenar et al. 2020b). Contemporary evolution models, which use modern mass-loss prescriptions, generally struggle to produce the bulk of apparently single WR stars in low-Z environments such as the SMC, suggesting that they may be binary products (Hainich et al. 2015, Shenar et al. 2016, Schootemeijer & Langer 2018). Indeed, short-period WR+O binaries with rapidly rotating O-star companions can indicate past interactions (e.g., Shenar et al. 2016, 2019). Although cWRs have current masses above ~8–16 $M_\odot$ (depending on their metallicity) and launch strong, optically thick stellar winds, sdOB stars are their equivalent at the low-mass end (see Heber 2009 for a review). These core-helium burning objects with masses $\lesssim$1 $M_\odot$ are thought to be stripped stars and are found in binaries with white dwarf, low-mass MS or OBe star companions (e.g., Schaffenroth et al. 2022; and see Section 5.3).

Stripped stars with masses in between have only recently been reported based on UV photometry and follow-up spectroscopy (Drout et al. 2023, Götberg et al. 2023), bridging sdOs with WRs and, thus, filling a long-standing gap in our understanding of postinteraction binaries. In particular, their current masses were estimated to be between 1 and 8 $M_\odot$, placing them in the intermediate-mass range between WRs and sdOBs. Interestingly, all systems with multiple epochs showed RV variations, indicating the presence of a companion.

5.3. Observational Constraints on Mass Gainers

Mass gainers from stable RLOF are expected to be rejuvenated (potentially appearing as blue stragglers in star clusters; Schneider et al. 2015) and rapidly rotating because of the accreted angular momentum (how rapidly still remains an open question; see Section 3). Based on a rapid population-synthesis calculation, de Mink et al. (2013) found that the rotational velocity distribution of massive stars is strongly shaped by binary interactions.

Indeed, the observed rotational velocity distribution of single OB stars in 30 Dor is bimodal, with a majority of stars rotating with velocities around 100 km s^{-1} and a tail of high velocities, interpreted as a signature of previous interactions (Dufton et al. 2013, Ramírez-Agudelo et al. 2013). A similar distribution was reported for the young SMC cluster NGC 346 (Dufton et al. 2019). Ramírez-Agudelo et al. (2015) further found a lack of very rapidly rotating O-type primaries compared to single O-type stars, implying that prior interaction is required to produce such rapid rotators. Similar results were also reported for Galactic O-type stars in the IACOB survey (Holgado et al. 2022, Britavskiy et al. 2023). The observed rotational velocities of stars in the slightly older cluster NGC 330 were interpreted as having been shaped by previous binary interactions (Bodensteiner et al. 2023).

If the stripped primary subsequently explodes as a SN, the system may be disrupted, potentially creating a rapidly rotating runaway or walkaway star (e.g., Blaauw 1961, Renzo et al. 2019). The Galactic runaway star ζ Ophiuchi was reported as such (with a space velocity of 30 km s^{-1}; see, e.g., Renzo & Götberg 2021). On a larger scale, the fraction of rapidly rotating OBe runaways matches binary population synthesis calculations (Boubert & Evans 2018). Investigating runaways in the VFTS, Sana et al. (2022) interpreted a population of rapidly rotating but slowly moving stars as results of binary ejections, in contrast to slowly rotating but rapidly moving stars interpreted as ejections by dynamical processes. Britavskiy et al. (2023) found that almost 65% of apparently single fast-rotating O stars in IACOB are runaways.

Rapidly rotating classical OBe stars were proposed to be interaction products (see Section 3). Theoretical models agree that forming OBe stars according to this channel is feasible (e.g., van Bever & Vanbeveren 1997, Shao & Li 2014, Hastings et al. 2021), but the predicted number of OBe stars varies from a few to basically 100%. The numbers depend strongly on model assumptions and uncertain interaction physics, such as the mass-transfer efficiency or the reaction of the accretor. Another open question is how close to critical rotation OBe stars are (Rivinius et al. 2013). If the binary channel dominates Be star formation, their multiplicity properties would be fundamentally different from normal OB stars. First, there should be no Be+MS binaries (unless they were with a third companion in an initial triple system), and second, their companions should be stripped stars or compact objects. In some cases, a massive enough companion might have exploded, potentially disrupting the system.

Several well-known Be stars were proposed to be in binaries with an evolved companion. One example is the first Be star ever described, γ Cassiopeiae, which is in a long-period binary system (e.g., Harmanec et al. 2000).[4] Despite its brightness and various observational campaigns with different techniques, it remains debated if the companion is a white dwarf, a helium star, or an NS (e.g., Langer et al. 2020a, and references therein).

The detection of stripped sdOB companions to Be stars further matches expectations of the binary channel. Given the temperatures and radii of those stars, they are faint in the optical and mostly detected in the UV (e.g., Gies et al. 1998; Peters et al. 2013; Wang et al. 2018, 2021, 2023).

[4] γ Cas also shows hard, moderately strong X-ray emission (Mason et al. 1976), making it the prototype of the so-called class of γ Cas stars (see, e.g., Nazé et al. 2022 for a recent compilation).

In a handful of cases, there is a direct signature of the sdO star in the optical spectrum (e.g., in ϕ Persei or FY Canis Majoris; Poeckert 1981, Rivinius et al. 2004), or an observable change in the Be disk induced by the presence of the hot companion can be seen (e.g., in o Puppis; Koubský et al. 2012). A handful of such systems were also detected through interferometry (e.g., the first Be+sdB system κ Dra; Klement et al. 2022).

5.4. Thermally Contracting Stripped Stars

Recently, a new type of OBe binary was reported in a brief evolutionary phase in between mass transfer and the OBe+sdOB phase, in which the stripped star has not yet contracted and is still similarly bright in the optical as the mass accretor, the Be star (see **Figure 4**). The first such systems reported were LB-1 (e.g., Irrgang et al. 2020, Shenar et al. 2020a) and HR 6819 (e.g., Bodensteiner et al. 2020b, El-Badry & Quataert 2021). Initially they were reported as binary or triple systems hosting a BH (Liu et al. 2019, Rivinius et al. 2020), mainly because of two observational characteristics: first, in contrast to sdOB systems, the optical spectrum is dominated by the narrow-lined stripped star showing large RV amplitudes indicative of a high mass ratio (in LB-1, the Be companion could only be revealed by spectral disentangling; Shenar et al. 2020a). Second, assuming the mass of the narrow-lined star, which appears like a normal B-type star, from a comparison to single-star evolutionary tracks leads to a very high mass of the unseen object. Given the proximity and brightness of HR 6819, the stripped star and Be companion with its disk could be resolved interferometrically (Frost et al. 2022). It was shown that the spectroscopic (and actual) masses of the stripped stars in LB-1 and HR 6819 are only $\lesssim 1\,M_{\odot}$, and their companions are rapidly rotating Be stars with masses around 6 $M_{\odot}$.

Other systems were thereafter detected with a similar signature but in which the mass gainer currently shows no emission lines, for example, the still uncertain, highly debated case of NGC 1850 BH1 (Saracino et al. 2022, 2023; El-Badry & Burdge 2022). Additional systems interpreted to have more massive stripped, bloated companions are VFTS 291 (Villaseñor et al. 2023), SMCSGS-FS 69 (Ramachandran et al. 2023), and AzV 476 (Pauli et al. 2022). Similarly, γ Col was recently reported as the stripped core of a more massive star in which no signature of a companion was detected (Irrgang et al. 2022).

These thermally contracting systems provide a critical snapshot of binary systems right after the interaction occurred (see **Figure 5**). A common feature is their mass ratios ($q = 5$ for LB-1, and $q \sim 15$ for HR 6819), which were reported to require conservative mass transfer. Although those systems are in a short evolutionary phase, they are more easily detectable with common observing techniques than their subsequent, longer-lived evolutionary stage [OB(e)+sdOB/WR systems] because of the higher optical brightness of the stripped star. El-Badry & Quataert (2021) also showed that their luminosity is not purely powered by contraction but also by shell-helium burning. This extends the lifetime of the contraction phase beyond the thermal timescale, making their observation more likely.

Another stripped star in a later evolutionary stage is the helium supergiant υ Sagittarius (Gilkis & Shenar 2023), which was reported to be in a currently interacting binary system during a second phase of mass transfer (see also Laplace et al. 2020). The more luminous primary was proposed to be stripped of the remainder of its hydrogen envelope, whereas the accretor is a rapidly rotating B-type star. The stripped primary of υ Sag is also included in **Figure 5** (the evolutionary tracks do not include this second phase of mass transfer).

The aforementioned systems form an evolutionary sequence (**Figure 5**) of recently stripped stars with OBe companions that later contract and appear as sdOB+OBe binaries during core-helium burning. Observationally, the recently stripped, contracting stars look like normal B-type

MS stars. This is in contrast to expected surface abundances of stripped stars, which are thought to be dominated by helium (Götberg et al. 2017, Schürmann et al. 2022). A potential explanation for the hydrogen-rich surface is that they have reaccreted hydrogen-rich material from the Be star decretion disk (Bodensteiner et al. 2020b). So far, a common characteristic of mass gainers is their rapid rotation. The lack of emission lines in some of the potential mass-gainer companions could simply be related to the transient nature of the Be phenomenon (e.g., Rivinius et al. 2013). The detection of more such systems will allow researchers to better constrain mass-transfer physics, the response of the accretor, and how close to the critical velocity it is spun up.

6. SINGLE- AND DOUBLE-DEGENERATE BINARIES

Once one of the components in a massive binary undergoes core collapse, it can produce an NS or BH (see Heger et al. 2023 for a recent review). The mapping between pre-explosion properties and the type and mass of the compact object depends on the physics of the SN process (or lack thereof). A common method used to assess the postexplosion outcome is the compactness parameter, taken as a ratio between the mass and the radius at a specific mass coordinate (O'Connor & Ott 2011). Stars with higher compactness in their central regions are expected to collapse into a BH. Stellar evolution calculations done until core collapse consistently show that, based on their compactness as well as other metrics, the boundary between NSs and BHs is not a simple mass threshold but rather consists of "islands" of explodability (Ugliano et al. 2012, Sukhbold & Woosley 2014, Sukhbold et al. 2016). Schneider et al. (2023) suggests that these variations in explodability lead to peaks in the mass distribution of BHs observed in GW sources. Furthermore, simulations indicate that stripping in a binary system shifts the range of initial masses that result in BHs upward, lowering predicted rates of binary BH mergers (Laplace et al. 2021, Schneider et al. 2021). Predicting the nature and mass of a compact remnant from its pre-explosion properties remains uncertain, and it was remarked that compactness might not be a good metric for explodability (e.g., Burrows et al. 2020).

Whether or not the compact object remains bound to its companion depends on the total mass ejected and the kick imparted onto it. Observed proper motions of isolated NSs have been used to assess the distribution of kick velocities (Hobbs et al. 2005) and are often utilized in both rapid and detailed evolutionary calculations. However, considering only isolated pulsars is biased toward the strongest kicks (e.g., O'Doherty et al. 2023), which can lead to an overestimate of unbound post-SN systems in population synthesis. Isolated BHs can be detected through lensing of their background stars, with a recent first detection (although data could also support a NS as the lens; Lam et al. 2022, Sahu et al. 2022). Data on isolated BHs are thus insufficient to estimate BH kick distributions, and instead BHs in X-ray binaries have been the standard method to determine BH kicks (e.g., Atri et al. 2019), showing support for both strong ($>50\,\mathrm{km\,s^{-1}}$) and weak kicks at birth. One weakness of the methods that use low-mass X-ray binaries to determine kicks is that they can only constrain the velocity imparted on the system at birth and not the magnitude of the kick imparted onto the BH itself.

If the binary remains bound after the formation of the first or second compact object, and if the end result is not a binary BH, we can use electromagnetic observations to infer its orbital parameters, serving as a laboratory of the SN process. A detailed understanding of the intrinsic population of single-degenerate binaries is also crucial as an anchor point to constrain evolutionary models. Tauris et al. (2017) recently provided an extensive review on binary NSs, including their formation and intermediate stages. Thus, we only provide a brief overview of NSs in massive binaries and focus our discussion on the properties of BH-HMXBs as well as the recently identified category of inert BHs (corresponding to BH binaries wide enough that little mass is transferred and no

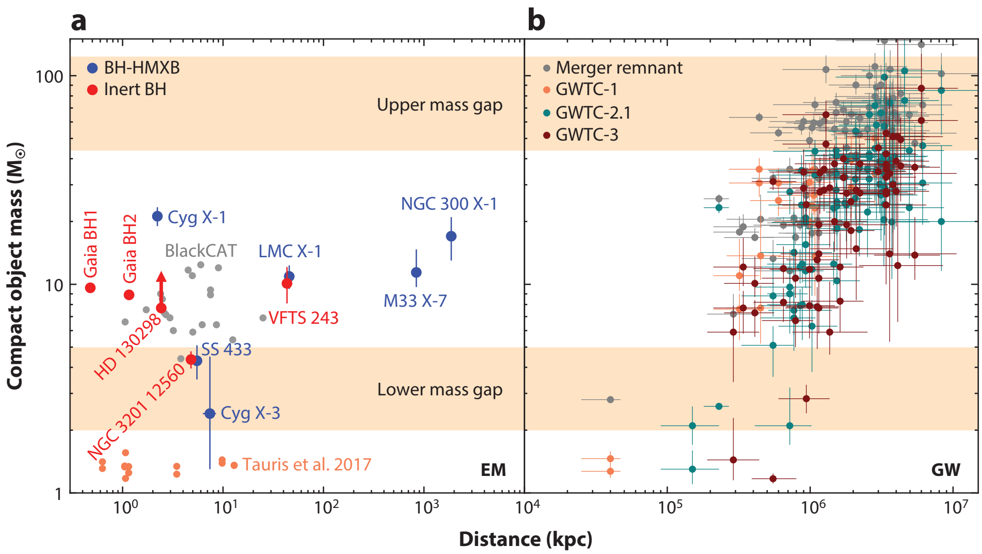

Figure 6

(*a*) Masses and distances to BH-HMXBs and inert BHs with measured dynamical masses. Also shown are the masses of low-mass X-ray transients with dynamical mass estimates from the BlackCAT catalog (Corral-Santana et al. 2016) and the masses of binary NSs collected by Tauris et al. (2017). (*b*) Masses of merging compact objects detected through GW emission. Representative bands are shown for the potential mass gap between NSs and BHs at around 2–5 $M_\odot$ and for the upper mass gap due to pair-instability SNe (data taken from Marchant et al. 2019). Abbreviations: BH, black hole; EM, electromagnetic; GW, gravitational wave; GWTC, Gravitational Wave Transient Catalogue; HMXB, high-mass X-ray binary; NS, neutron star; SN, supernova.

accretion disk is formed). A compilation of masses and distances of NSs and BHs in massive binaries is shown in **Figure 6**, including also GW observations. The detection of BHs through GWs has significantly outnumbered the electromagnetic sources for which we have mass constraints, but the population of inert BHs could grow by orders of magnitude in the coming decade (see Section 6.3).

6.1. Neutron Stars in Massive Binaries

BeXRBs are composed of a compact object that is fed from the decretion disk of its companion Be star (Negueruela 1998, Okazaki & Negueruela 2001; see Reig 2011 for a review). Only one system has been claimed to contain a BH rather than an NS (Casares et al. 2014), but its status is currently contested with the compact object potentially being a stripped helium star instead (Rivinius et al. 2022, Janssens et al. 2023a). Assuming that a previous mass-transfer phase circularized the orbit before the SN, the eccentricity distribution of BeXRBs is indicative of a subpopulation that underwent small kicks at NS formation (Pfahl et al. 2002). One explanation for this is the occurrence of electron capture SNe rather than iron-core collapse SNe (Podsiadlowski et al. 2004). The masses of Be stars in X-ray binaries have been used to argue that they underwent an efficient mass-transfer process (Vinciguerra et al. 2020), but masses for Be stars are typically inferred from their spectral type, which carries significant uncertainty.

In OB+NS systems, after the OB star finishes its MS evolution, it expands and fills its own Roche lobe (see **Figure 4**). Owing to the large mass ratio, this most likely results in CE evolution, forming a compact stripped star+NS system, or instead merging. The outcome of a compact object merging with a stellar companion is uncertain, with possible outcomes being a stable Thorne–Zytkow object (Thorne & Zytkow 1975; see Farmer et al. 2023b for a recent picture) or a SN explosion (Chevalier 2012, Metzger 2022). Systems that survive CE and have stripped stars with masses $\lesssim 5\,M_\odot$ can undergo an additional phase of mass transfer after core helium depletion, which is referred to as Case BB mass transfer[5] (Tauris et al. 2015). This mass-transfer phase can leave an almost stripped helium core, producing SNe with $\lesssim 0.1\,M_\odot$ of ejecta and potentially small kick velocities (Moriya et al. 2017).

If the binary remains bound after the second SN, a double-degenerate binary is produced. NSs detectable as radio pulsars in binaries provide an accurate probe of their radial motion through measurements of variations in pulse time arrival. It was through timing of the first binary pulsar (Hulse & Taylor 1975) that GWs were first measured indirectly (Taylor et al. 1979; see Weisberg et al. 2010 for results with over three decades of timing data). Another remarkable case is the double pulsar (Kramer et al. 2006, 2021), where the detection of multiple post-Newtonian effects in the orbit allows the measurement of the individual pulsar masses to better than one part in ten thousand. Currently, there are over 20 binary NSs detected (see Bernadich et al. 2023 for a recent collection), and the sample is expected to grow by up to an order of magnitude with the advent of the Square Kilometer Array (Keane et al. 2015). Even though binary NSs are usually discussed in the context of isolated binary evolution, it is important to consider alternative scenarios. Andrews & Mandel (2019) suggested that the current sample contains a subpopulation that is inconsistent with binary evolution and could have formed through dynamical processes.

6.2. Black Hole High-Mass X-Ray Binaries

The X-ray flux of young star-forming galaxies without active galactic nuclei is dominated by HMXBs. The *Chandra X-ray Observatory* telescope has played a pivotal role in their study, allowing for the observation of X-ray binaries in galaxies beyond the local group (see Gilfanov et al. 2023 for a recent review). The brightest of these sources, with luminosities exceeding 10^{39} erg s^{-1}, are referred to as ULXs (Long & van Speybroeck 1983; see Kaaret et al. 2017 for a recent review). ULXs exceed the Eddington limit for a 10-$M_\odot$ BH, in some cases by over an order of magnitude, and as such they have been suggested to hold intermediate-mass BHs. This need not be the case if there is significant beaming of radiation, which King et al. (2001) argues would be true for rapid thermal-timescale mass-transfer phases onto compact objects. Even more contrary to the idea that ULXs host intermediate-mass BHs, the discovery of X-ray pulsations in some systems allowed a clear identification of their compact object accretors to be NSs (Bachetti et al. 2014). A clear identification of a BH accretor in a ULX is more elusive, but within our own Galaxy, it is suggested that the microquasar SS 433 (which hosts a BH) would appear as a ULX if observed from a different angle (Begelman et al. 2006).

For extragalactic X-ray binaries, spectroscopic follow-up that would allow the measurement of RVs and an estimate of the compact object mass is challenging. Even when spectral features associated to the donor are detected, observed RV variations might not follow the orbital motion. Such is the case for IC10 X-1, which contains a WR star orbiting a compact object with a period of 35 h. RV variations of the WR star indicated that IC10 X-1 hosts the most massive stellar-mass BH known (Prestwich et al. 2007, Silverman & Filippenko 2008). However, Laycock et al. (2015) showed that the phase of the RV variability was inconsistent with eclipses in the system and, as such, did not trace the orbital motion of the WR star, making the nature of the compact object unclear. Important adjustments have also been made to the measured masses of the BHs in

[5] Consistent nomenclature would use the name case BC for this phase, as it happens after core helium depletion.

Table 2 Properties of BH-HMXBs and inert BHs[a]

Name	d (kpc)	P (days)	M_{CO} ($M_\odot$)	M_{comp} ($M_\odot$)	BH spin	References
BH-HMXBs						
Cyg X-1	$2.22^{+0.17}_{-0.18}$	5.60	21.2 ± 2.2	$40.6^{+7.7}_{-7.1}$	>0.9985	Miller-Jones et al. 2021
Cyg X-3	7.4 ± 1.1	0.200	2.4 ± 2.1	$10.3^{+3.9}_{-2.8}$	–	Singh et al. 2002, Zdziarski et al. 2013, McCollough et al. 2016
NGC 300 X-1	1870^{+115}_{-108}	1.37	17 ± 4	26^{+7}_{-5}	–	Rizzi et al. 2006, Crowther et al. 2010, Binder et al. 2021
M33 X-7	840^{+27}_{-28}	3.45	$11.4^{+3.3}_{-1.7}$	38^{+22}_{-10}	0.84 ± 0.05	Pietsch et al. 2006, Liu et al. 2010, Gieren et al. 2013, Ramachandran et al. 2023
LMC X-1	45.59 ± 0.09	3.91	10.91 ± 1.41	31.79 ± 3.48	$0.92^{+0.05}_{-0.07}$	Gou et al. 2009, Orosz et al. 2009, Pietrzyński et al. 2019
SS 433	5.5 ± 2.2	13.1	4.3 ± 0.8	12.3 ± 3.3	–	Blundell & Bowler 2004, Hillwig & Gies 2008
Inert BHs						
VFTS 243	45.59 ± 0.09	10.4	10.1 ± 2.0	25.0 ± 2.3	–	Pietrzyński et al. 2019, Shenar et al. 2022b
HD 130298	$2.425^{+0.08053}_{-0.07507}$	14.6	$>7.7 \pm 1.5$	24.2 ± 3.8	–	Mahy et al. 2022b
Gaia BH1	0.477 ± 0.004	186	9.62 ± 0.18	0.93 ± 0.05	–	El-Badry et al. 2023b
Gaia BH2	1.16 ± 0.02	128	8.94 ± 0.34	1.07 ± 0.19	–	El-Badry et al. 2023a
NGC 3201 12560	4.8	167	4.36 ± 0.41	0.81 ± 0.05	–	Giesers et al. 2018

Abbreviations: BH, black hole; HMXB, high-mass X-ray binary; NS, neutron star.
[a]The columns give the distance, d; orbital period, P; mass of the compact object, M_{CO}; mass of the companion star, M_{comp}; and spin. Cyg X-3 could potentially have an NS instead of a BH. The error on the orbital period for all systems is below 1%. Spins of black holes indicated with a dash (–) are unconstrained.

Cyg X-1 and M33 X-7. A more accurate distance determination for Cyg X-1, placing it further away from us, has increased the mass estimate of its donor by ~30%, leading to a corresponding increase on its estimated BH mass (Miller-Jones et al. 2021). For M33 X-7, detailed spectroscopic modeling of its donor star has instead lowered the donor mass estimate by ~30%, leading to a lower mass estimate for its BH (Ramachandran et al. 2022).

In the presence of an accretion disk around the BH, it is also possible to constrain its dimensionless spin (see Belczynski et al. 2021 for an overview of methods, as well as caveats). **Table 2** lists the three known BH-HMXBs with spin estimates, all of which are high. For M33 X-7, Ramachandran et al. (2022) argued that the lowered mass estimate on the BH would lower its measured spin from 0.84 ± 0.05 (Liu et al. 2010) down to ~0.6. For both Cyb X-1 and LMC X-1, the spin of the BH is near critical rotation. The origin of the high spin of these BHs is unclear. It has been suggested that the source of the angular momentum in the BH progenitor came from tidal synchronization during an earlier stage of mass transfer (Valsecchi et al. 2010, Qin et al. 2018) or from a failed SN, where some mass expanded and gained angular momentum from the orbit before falling back into the newly formed BH (Batta et al. 2017). Understanding the origin of spin in BH-HMXBs is crucial to understanding their potential link to GW sources, which are mostly observed to have low spins (see the discussion by Fishbach & Kalogera 2022). If BH-HMXBs inherit their spins from tidal coupling, longer-period systems could potentially exhibit lower spins, but it is unclear at which orbital period the BH would become X-ray inactive.

To get detectable X-ray fluxes in BH binaries, the BH not only has to accrete sufficient mass but also an accretion disk must form (Shapiro & Lightman 1976). Taking this into account, Vanbeveren et al. (2020) suggested that if the known WR+O binary systems in the Solar Neighborhood would evolve to become BH+O binaries, there should be over 100 BH-HMXBs within a few kiloparsecs of the Sun. A solution to that discrepancy would require most WR+O binaries to undergo a SN explosion and form an NS or form a BH with a strong kick that unbinds the system. Sen et al. (2021) improved upon the model for disk formation by Vanbeveren et al. (2020) and showed that owing to the fast winds of OB stars, only the closest OB+BH binaries would be observed as X-ray sources. Similarly, Hirai & Mandel (2021) suggested that tidal deformation in near-Roche-filling binaries leads to slow wind outflows through the vicinity of the L1 point, which can efficiently be captured by the BH and produce an accretion disk. If only near-Roche-filling systems can form discs around BHs, then WR+O star systems can still primarily evolve toward BH+O star binaries without being in conflict with the low number of observed BH-HMXBs. The vast majority of BHs with massive companions would then be inactive in X-rays.

6.3. Inert Black Holes

Recent work on the proposed population of long-period BHs that do not form accretion disks has referred to them as "quiescent" or "dormant." However, this denomination can be confused with nomenclature used for X-ray active binaries, which can undergo periods of X-ray inactivity while still containing an accretion disk. We instead adopt the term "inert" for these BHs to indicate that other than their gravitational influence on their companions, we do not expect them to become X-ray active in the near future. Using detailed population synthesis calculations, Langer et al. (2020b) has suggested that ∼3% of OB binaries contain BH companions, and almost all would be inert.

There are three main methods proposed to identify inert BHs in binaries. In low-mass BH binaries, ellipsoidal variability near Roche filling for the donor star can be identified through photometric measurements (e.g., Gomel et al. 2021), although with a massive star donor it is expected that wind mass transfer would already make it active at this stage. Alternatively, the reflex motion of the companion star can be determined either through astrometry and/or by measuring its RV through spectroscopy. Currently, it is only via spectroscopy and astrometry that confident detections have been made.

In the context of the *Gaia* mission, multiple studies pointed out the possibility of detecting hundreds to thousands of inert Galactic BHs in binaries (Breivik et al. 2017, Mashian & Loeb 2017, Yalinewich et al. 2018, Yamaguchi et al. 2018, Wiktorowicz et al. 2019, Chawla et al. 2022, Janssens et al. 2022). Although this was expected to happen with *Gaia*'s DR3, the stringent criteria that were placed on the data in order to release orbital solutions excluded almost all massive stars (Janssens et al. 2023b). Current discoveries have instead been made in the low-mass regime, with El-Badry et al. (2023a,b) reporting two confident detections of ∼9-$M_\odot$ BHs orbiting ∼1-$M_\odot$ stars (one of them also independently reported by Chakrabarti et al. 2023).

Spectroscopic measurements have allowed the first identification of inert BHs with massive companions. As part of the TMBM survey, Shenar et al. (2022a) followed up on the 51 apparent SB1 systems using spectral disentangling to exclude the presence of a second luminous component. This allowed them to discover VFTS 243 (Shenar et al. 2022b), a binary consisting of a 25 ± 2.3-$M_\odot$ O star and a 10 ± 2-$M_\odot$ BH companion in a near-circular orbit ($e = 0.017 \pm 0.012$). Similarly, Mahy et al. (2022b) studied a sample of 32 Galactic SB1 stars and identified HD 130298 as an O+BH system, with masses similar to those of VFTS 243 but an eccentricity $e = 0.457 \pm 0.007$. Contrary to BH-HMXBs, where large filling factors would lead to rapid circularization, the eccentricity in inert BHs provides a direct constraint on the SN kick at their formation. Shenar et al. (2022b) have argued that the BH in VFTS 243 most likely formed with a weak kick and $<1\,M_{\odot}$ of ejecta. Spectroscopic observations have also allowed for the detection of an inert BH with a low-mass companion (Giesers et al. 2018), as well as two additional candidates (Giesers et al. 2019, Mahy et al. 2022b, Shenar et al. 2022a).

Gravitational Wave Transient Catalogues (GWTCs): catalogs of detected compact object mergers released by the LIGO–Virgo–KAGRA collaboration

7. GRAVITATIONAL WAVE SOURCES

GW observations are emerging as a very fertile ground to study the evolution of massive and very massive stars. They are also very rapidly evolving, and as such, our objective here is not to provide a thorough review of the current state of this field. Rather, we aim to discuss the prospects of future GW observations as well as the binary processes that are thought to contribute to the observed sample.

7.1. Observations of Gravitational Wave Sources

Second generation GW observatories (including advanced LIGO and advanced Virgo and KAGRA) are currently on their third observing round (Abbott et al. 2020). The teams that develop each of these instruments are assembled into the LIGO–Virgo–KAGRA collaboration and, up to the moment of writing, have released almost a hundred detections, which are compiled in the Gravitational Wave Transient Catalogues (GWTCs; Abbott et al. 2023a). For any given compact object merger, the three best-constrained quantities are the chirp mass, the mass ratio,[6] and the effective spin, defined, respectively, as:

$$\mathcal{M} = \frac{(m_1 m_2)^{3/5}}{(m_1+m_2)^{1/5}}, \quad q = \frac{m_2}{m_1}, \quad \chi_{\rm eff} = \frac{m_1\chi_1 + m_2\chi_2}{m_1 + m2}, \tag{6}$$

where χ_1 and χ_2 are the components of the dimensionless spin of each compact object that are aligned with the orbital angular momentum. The frequency evolution of the source provides a measurement of the redshifted chirp mass $(1+z)\mathcal{M}$, and to determine $\mathcal{M}$ one needs to make an assumption about the cosmology. Cases in which an associated electromagnetic transient is detected are of particular importance, as a separate redshift measurement allows for the use of GW sources as standard candles, as was the case for GW170817 (Abbott et al. 2017). The chirp mass is directly derived by the frequency evolution of the binary, so for binaries that undergo many cycles in-band it can be accurately determined. For instance, the error on the chirp mass for GW170817 was smaller than 0.5%. Most measurements of q and $\chi_{\rm eff}$ show a significant degeneracy with current detector sensitivity, which can make it difficult to differentiate the nature of the merging compact objects (Hannam et al. 2013). In some sources, additional information has been obtained by measuring precession (Hannam et al. 2022, Varma et al. 2022) as well as ringdown frequencies (Abbott et al. 2021).

The long-term prospects of GW astrophysics are certainly exciting. As the measured strain is proportional to the inverse of the luminosity distance (rather than an inverse square dependence as for electromagnetic waves), detector improvements greatly increase the volume of sensitivity. This may result in $\sim 10^4$ detections by the end of the decade (Baibhav et al. 2019). With expected sensitivity, third-generation detectors will probe the Universe down to the redshift of the formation of the first stars (Hall & Evans 2019), making GW mergers the best characterized

[6] Mass ratios in GW observations are normally defined as the ratio between the least and the most massive components, and as such, they are smaller than unity.

population of stellar-mass compact objects. Space-based missions such as the LISA (*Laser Interferometer Space Antenna*) will operate at lower frequencies and allow for multiband detections of stellar-mass merging binary BHs (Sesana 2016).

Besides providing a probe into new astrophysical environments, two aspects of GW science make it very interesting to contrast observations against the theory of binary evolution. On one hand, detector biases are very well understood, allowing for a transparent determination of intrinsic source properties. Owing to the limited number of observations, at the moment most distribution properties are determined using parameterized models that contain expected features such as the lower and upper BH mass gaps (Abbott et al. 2023b), but reliance on such models will decrease as the number of detections increases. On the theoretical side, given a model that produces the rate of formation of double compact objects (including their masses, separations, and spins), it is straightforward to provide expected rates of observation for specific detectors, as the time it takes for two compact objects to merge is easily calculable from general relativity (Peters 1964).

7.2. Binary Formation Channels of Gravitational Wave Sources

Although one could expect the natural formation scenario of a merging binary BH to involve the evolution of two stars in a binary system, a wide variety of processes that do not involve binary interaction are being considered (see Mandel & Farmer 2022 for an overview of some of the proposed channels). The relative contribution of different formation scenarios to the observed population is still uncertain, although comparison of predicted distributions to observations suggests that multiple processes contribute to it (e.g., Zevin et al. 2021). One important thing to keep in mind is that evolutionary paths toward a merging compact object are a rare outcome of massive-star evolution. Currently, measured merger rates at redshift zero, in units of $\mathrm{Gpc}^{-3}\ \mathrm{year}^{-1}$, reside in the ranges of 10–1,700, 7.8–130, and 16–61 for NS+NS, NS+BH, and BH+BH mergers (Abbott et al. 2023b), respectively. In contrast, the rate for core-collapse SNe is on the order of $10^5\ \mathrm{Gpc}^{-3}\ \mathrm{year}^{-1}$. Independent of the formation process, the main challenge to form a GW source is that the resulting binary BH needs to remain in a very compact orbit. For a circular compact object binary with a given orbital period and chirp mass, the time it takes for GWs to produce a merger is (Peters 1964):

$$t_{\mathrm{delay}} = 11.9\,\mathrm{Gyr}\left(\frac{P}{5\,(\mathrm{days})}\right)^{8/3}\left(\frac{\mathcal{M}}{30\,\mathrm{M}_\odot}\right)^{-5/3}. \qquad 7.$$

This implies that massive binaries that evolve to form merging binary BHs necessarily interact during their lifetimes, and they need not only survive to form a compact object binary but also finish their evolution in a short-period orbit.

The classic formation channel used to explain their formation is CE evolution. Shortly after Paczynski (1976) proposed CE as the formation scenario for cataclysmic variables, van den Heuvel (1976) suggested that CE could explain the formation of the Hulse–Taylor binary pulsar, whereas Tutukov & Yungelson (1993) argued it could also produce binary BHs (see Bavera et al. 2021 for a recent overview). An alternative scenario considers the case in which both stars in a (near-)contact binary evolve chemically homogeneously (Mandel & de Mink 2016, Marchant et al. 2016) and form a binary BH. Chemically homogeneous evolution can also lead to the formation of merging BH+NS systems (Marchant et al. 2017). The third formation process that is commonly considered to form merging binary BHs is stable mass transfer (van den Heuvel et al. 2017), where a short-period binary is formed through nonconservative mass transfer from a star onto the first formed BH in the system. Picco et al. (2023) have suggested that stable mass transfer can also naturally produce NS+BH mergers, and that the mechanism is robust against uncertainties on the angular momentum budget of binary outflows. Current work suggests that population synthesis studies have systematically overestimated the contribution of the CE channel to the formation of merging binary BHs, owing to issues with adopted binding energies and criteria for unstable mass transfer (Gallegos-Garcia et al. 2021, Klencki et al. 2021, Marchant et al. 2021, Olejak et al. 2021). One channel that is not often discussed is that of pop III evolution, in which case the absence of metals is expected to lead to much smaller stellar radii, making it easier to form compact binaries by the end of their evolution (Kinugawa et al. 2014).

Many studies have performed population synthesis (using both detailed and rapid codes) to compute the rates and distributions of compact object mergers. Mandel & Broekgaarden (2022) made a compilation of published rate predictions that was not restricted to only binary evolution, illustrating how individual channels not only have uncertainties of over an order of magnitude but that predictions from different groups can also have order-of-magnitude discrepancies. This is not entirely surprising, because predicting merging compact objects requires an understanding of all phases of massive binary evolution coupled with the metallicity-dependent star-formation history. Even for individual systems, different codes can produce wildly different outcomes for both single-star evolution (Romagnolo et al. 2023) and binary evolution (Belczynski et al. 2022). Moving forward will require collaboration within different research groups to identify the sources of these modeling discrepancies, as well as to define the different characteristic features of the distribution of merging compact objects that remain invariant independent of physical uncertainties (van Son et al. 2023).

8. CONCLUSIONS

In the past few decades, the field of massive binary evolution has grown significantly in terms of interest and scientific advances. This was driven first and foremost by large-scale spectroscopic observations, high-quality continuous photometric monitoring, and high-precision astrometric surveys. A consensus has emerged that binary evolution dominates the lives of massive stars, providing exciting new evolutionary pathways but also complicating our theoretical description of stellar evolution. In recent years, massive stars gained further visibility due to the detection of GWs, which opened a new window to constrain potential end products of massive star evolution. As a conclusion, we provide below summary points as well as future issues that we expect will shape the field in the coming decade.

SUMMARY POINTS

1. A game changer in recent years has been large-scale surveys with well-understood biases, not only for electromagnetic observations in terms of spectroscopic, photometric, or astrometric surveys but also in terms of gravitational wave (GW) detections, for which detection biases are well constrained. These have corroborated the finding that binary interactions dominate massive star evolution.
2. Observations tentatively indicate that the multiplicity properties of OB stars, both binary fractions and orbital parameter distributions, are universal across the probed metallicity environments of the Milky Way, Large Magellanic Cloud, and Small Magellanic Cloud.
3. Theoretical models of binary evolution rely on three distinct types of calculations, including 3D hydrodynamical codes, 1D stellar-evolution calculations, and rapid semianalytical approximations. Each of these play a critical role.
4. Observational evidence is growing that a majority of rapidly rotating stars, in particular OBe stars, can be explained as accretors in previous binary interactions.

5. In recent years, our picture of postinteraction products has been expanded to include massive stripped stars [closing the previous gap between sdOs and Wolf–Rayets (WRs)] as well as thermally contracting objects right after mass stripping. These provide a novel perspective about the mass transfer process.
6. Inert black holes (BHs) without accretion disks or detectable X-ray radiation have been identified in binary systems. These extend the known population of BHs to longer periods, and a much larger population will potentially be unveiled in the coming years.
7. The number of GW observations has surpassed that of compact objects with dynamical masses measured from electromagnetic radiation. They provide a new window into massive star evolution, but their formation processes remain unclear.

FUTURE ISSUES

1. The multiplicity fractions and orbital parameters of key objects such as OBe stars, WR stars, or blue supergiants remain poorly understood. Constraining these can provide us with important new insights on their evolutionary status and connection.
2. Stellar evolution models still rely on simplified assumptions regarding how conservative mass transfer is and the dynamics of outflows from binary systems. Narrowing down this uncertainty will require careful studies that combine detailed hydrodynamical simulations with long-term evolutionary calculations.
3. Increased detections of inert BHs will provide a critical anchor point for binary evolution models. They will also give novel constraints on the supernova (SN) process and, in particular, potential kicks imparted onto the BH at birth. This will also require a clear understanding of the pre-SN binary properties, in particular, the eccentricity and period distribution of WR+OB binaries.
4. Recent observations indicate that triple- and higher-order multiple systems are common, and even more so for more massive stars. These could be important probes of the star-formation process and play a crucial role by inducing binary interactions through dynamical processes.
5. It is critical to benchmark binary evolution models against each other to clearly identify which physical assumptions lead to discrepant results.
6. It is also important to keep in mind that significant uncertainty still exists regarding massive single-star evolution, which translates directly into binary evolution. In particular, the radial evolution of stars near the Eddington limit is poorly understood.
7. Recent space missions like the *James Webb Space Telescope*, and new instrumentation on upcoming 40-m-class telescopes, such as HARMONI (High Angular Resolution Monolithic Optical and Near-infrared Integral field spectrograph) or MICADO (Multi-AO Imaging CamerA for Deep Observations) at the European Space Observatory's Extremely Large Telescope (first light expected before the end of the decade), will push our understanding of massive-star evolution to lower metallicity, for example, by resolving individual stars in distant stellar populations.

8. GW astrophysics will provide an unparalleled perspective on the end stages of massive-star evolution. However, significant work remains to be done to understand the role of binary evolution in the formation of GW sources.

DISCLOSURE STATEMENT

The authors are not aware of any affiliations, memberships, funding, or financial holdings that might be perceived as affecting the objectivity of this review.

ACKNOWLEDGMENTS

The authors thank Tomer Shenar and Alina Istrate for always insightful discussions and comments on the manuscript. We also thank Hugues Sana, Fabian Schneider, Lee Patrick, Tom Maccarone, Jim Fuller, and the scientific editor Eliot Quataert for their useful feedback. P.M. acknowledges support from the Fonds Wetenschappelijk Onderzoek senior postdoctoral fellowship (12ZY523N).

LITERATURE CITED

Aasi J, Abbott BP, Abbott R, et al. 2015. *Classical Quantum Gravity* 32(7):074001
Abbott BP, Abbott R, Abbott TD, et al. 2016. *Phys. Rev. Lett.* 116(6):061102
Abbott BP, Abbott R, Abbott TD, et al. 2017. *Phys. Rev. Lett.* 119(16):161101
Abbott BP, Abbott R, Abbott TD, et al. 2020. *Living Rev. Relativity* 23:3
Abbott R, Abbott TD, Abraham S, et al. 2021. *Phys. Rev. D* 103(12):122002
Abbott R, Abbott TD, Acernese F, et al. 2023a. *Phys. Rev. X* 13(4):041039
Abbott R, Abbott TD, Acernese F, et al. 2023b. *Phys. Rev. X* 13:011048
Abdul-Masih M, Escorza A, Menon A, et al. 2022. *Astron. Astrophys.* 666:A18
Abdul-Masih M, Sana H, Conroy KE, et al. 2020. *Astron. Astrophys.* 636:A59
Abdul-Masih M, Sana H, Hawcroft C, et al. 2021. *Astron. Astrophys.* 651:A96
Abdul-Masih M, Sana H, Sundqvist J, et al. 2019. *Ap. J.* 880(2):115
Abt HA, Gomez AE, Levy SG. 1990. *Ap. J. Suppl.* 74:551–73
Abt HA, Levy SG. 1978. *Ap. J. Suppl.* 36:241–58
Acernese F, Agathos M, Agatsuma K, et al. 2015. *Classical Quantum Gravity* 32(2):024001
Agrawal P, Hurley J, Stevenson S, et al. 2020. *MNRAS* 497(4):4549–64
Aldoretta EJ, Caballero-Nieves SM, Gies DR, et al. 2015. *Astron. J.* 149:26
Almeida LA, Sana H, de Mink SE, et al. 2015. *Ap. J.* 812(2):102
Almeida LA, Sana H, Taylor W, et al. 2017. *Astron. Astrophys.* 598:A84
Andrews JJ, Mandel I. 2019. *Ap. J. Lett.* 880:L8
Asplund M, Grevesse N, Sauval AJ, Scott P. 2009. *Annu. Rev. Astron. Astrophys.* 47:481–522
Atri P, Miller-Jones JCA, Bahramian A, et al. 2019. *MNRAS* 489(3):3116–34
Baade D, Rivinius T, Pigulski A, et al. 2016. *Astron. Astrophys.* 588:A56
Bachetti M, Harrison FA, Walton DJ, et al. 2014. *Nature* 514(7521):202–4
Baibhav V, Berti E, Gerosa D, et al. 2019. *Phys. Rev. D* 100(6):064060
Banyard G, Sana H, Mahy L, et al. 2022. *Astron. Astrophys.* 658:A69
Barbá RH, Gamen R, Arias JI, Morrell NI. 2017. In *The Lives and Death-Throes of Massive Stars, Proc. IAU Symp. 329*, ed. JJ Eldridge, JC Bray, LAS McClelland, L Xiao, pp. 89–96. Cambridge, UK: Cambridge Univ. Press
Barnsley RM, Steele IA. 2013. *Astron. Astrophys.* 556:A81
Batta A, Ramirez-Ruiz E, Fryer C. 2017. *Ap. J. Lett.* 846(2):L15
Bavera SS, Fragos T, Zevin M, et al. 2021. *Astron. Astrophys.* 647:A153

Begelman MC, King AR, Pringle JE. 2006. *MNRAS* 370:399–404
Belczynski K, Done C, Lasota JP. 2021. arXiv:2111.09401
Belczynski K, Holz DE, Bulik T, O'Shaughnessy R. 2016. *Nature* 534(7608):512–15
Belczynski K, Kalogera V, Bulik T. 2002. *Ap. J.* 572:407–31
Belczynski K, Romagnolo A, Olejak A, et al. 2022. *Ap. J.* 925:69
Bellm EC, Kulkarni SR, Graham MJ, et al. 2019. *Publ. Astron. Soc. Pac.* 131(995):018002
Bernadich MCI, Balakrishnan V, Barr E, et al. 2023. *Astron. Astrophys.* 678:A187
Binder BA, Sy JM, Eracleous M, Christodoulou DM, Bhattacharya S, et al. 2021. *Ap. J.* 910:74
Blaauw A. 1961. *Bull. Astron. Inst. Neth.* 15:265–90
Blundell KM, Bowler MG. 2004. *Ap. J. Lett.* 616(2):L159–62
Bodensteiner J, Sana H, Dufton PL, et al. 2023. *Astron. Astrophys.* 680:A32
Bodensteiner J, Sana H, Mahy L, et al. 2020a. *Astron. Astrophys.* 634:A51
Bodensteiner J, Sana H, Wang C, et al. 2021. *Astron. Astrophys.* 652:A70
Bodensteiner J, Shenar T, Mahy L, et al. 2020b. *Astron. Astrophys.* 641:A43
Bodensteiner J, Shenar T, Sana H. 2020c. *Astron. Astrophys.* 641:A42
Boffin HMJ, Rivinius T, Mérand A, et al. 2016. *Astron. Astrophys.* 593:A90
Bordier E, Frost AJ, Sana H, et al. 2022. *Astron. Astrophys.* 663:A26
Borucki WJ, Koch D, Basri G, et al. 2010. *Science* 327(5968):977–80
Boubert D, Evans NW. 2018. *MNRAS* 477(4):5261–78
Braithwaite J, Spruit HC. 2004. *Nature* 431(7010):819–21
Breivik K, Chatterjee S, Larson SL. 2017. *Ap. J. Lett.* 850:L13
Breivik K, Coughlin S, Zevin M, et al. 2020. *Ap. J.* 898:71
Britavskiy N, Lennon DJ, Patrick LR, et al. 2019. *Astron. Astrophys.* 624:A128
Britavskiy N, Simón-Díaz S, Holgado G, et al. 2023. *Astron. Astrophys.* 672:A22
Brookshaw L, Tavani M. 1993. *Ap. J.* 410:719–31
Burki G, Mayor M. 1983. *Astron. Astrophys.* 124:256–66
Burrows A, Radice D, Vartanyan D, et al. 2020. *MNRAS* 491(2):2715–35
Casares J, Negueruela I, Ribó M, et al. 2014. *Nature* 505(7483):378–81
Cehula J, Pejcha O. 2023. *MNRAS* 524:471–90
Chakrabarti S, Simon JD, Craig PA, et al. 2023. *Astron. J.* 166:6
Chatzopoulos E, Frank J, Marcello DC, Clayton GC. 2020. *Ap. J.* 896:50
Chawla C, Chatterjee S, Breivik K, et al. 2022. *Ap. J.* 931(2):107
Chevalier RA. 2012. *Ap. J. Lett.* 752:L2
Chini R, Hoffmeister VH, Nasseri A, et al. 2012. *MNRAS* 424(3):1925–29
Clark JS, Lohr ME, Najarro F, et al. 2023. *MNRAS* 521(3):4473–89
Coe MJ, Kirk J. 2015. *MNRAS* 452:969–77
Conti PS. 1975. *Mem. Soc. R. Sci. Liege* 9:193–212
Corral-Santana JM, Casares J, Muñoz-Darias T, et al. 2016. *Astron. Astrophys.* 587:A61
Crowther PA. 2007. *Annu. Rev. Astron. Astrophys.* 45:177–219
Crowther PA, Barnard R, Carpano S, et al. 2010. *MNRAS* 403:L41–45
de Jager C. 1998. *Astron. Astrophys. Rev.* 8(3):145–80
de Mink SE, Belczynski K. 2015. *Ap. J.* 814:58
de Mink SE, Cantiello M, Langer N, et al. 2009. *Astron. Astrophys.* 497:243–53
de Mink SE, Langer N, Izzard RG, et al. 2013. *Ap. J.* 764(2):166
de Mink SE, Pols OR, Hilditch RW. 2007. *Astron. Astrophys.* 467(3):1181–96
de Mink SE, Sana H, Langer N, et al. 2014. *Ap. J.* 782:7
Dorda R, Patrick LR. 2021. *MNRAS* 502(4):4890–902
Drout MR, Götberg Y, Ludwig BA, et al. 2023. *Science* 382(6676):1287–91
Dsilva K, Shenar T, Sana H, Marchant P. 2020. *Astron. Astrophys.* 641:A26
Dsilva K, Shenar T, Sana H, Marchant P. 2022. *Astron. Astrophys.* 664:A93
Dsilva K, Shenar T, Sana H, Marchant P. 2023. *Astron. Astrophys.* 674:A88
Duchêne G, Kraus A. 2013. *Annu. Rev. Astron. Astrophys.* 51:269–310

Dufton PL, Evans CJ, Hunter I, et al. 2019. *Astron. Astrophys.* 626:A50
Dufton PL, Langer N, Dunstall PR, et al. 2013. *Astron. Astrophys.* 550:A109
Dunstall PR, Dufton PL, Sana H, et al. 2015. *Astron. Astrophys.* 580:A93
Eggleton PP. 1971. *MNRAS* 151:351–64
Eggleton PP. 1983. *Ap. J.* 268:368–69
Eggleton PP. 1996. In *The Origins, Evolution, and Destinies of Binary Stars in Clusters*, Vol. 90, *ASP Conf. Ser.*, ed. EF Milone, JC Mermilliod, pp. 257–69. San Francisco: ASP
El-Badry K, Burdge KB. 2022. *MNRAS* 511:24–29
El-Badry K, Quataert E. 2021. *MNRAS* 502(3):3436–55
El-Badry K, Rix HW, Cendes Y, et al. 2023a. *MNRAS* 521(3):4323–48
El-Badry K, Rix HW, Quataert E, et al. 2023b. *MNRAS* 518:1057–85
Eldridge JJ, Izzard RG, Tout CA. 2008. *MNRAS* 384(3):1109–18
Eldridge JJ, Stanway ER. 2022. *Annu. Rev. Astron. Astrophys.* 60:455–94
Eldridge JJ, Stanway ER, Xiao L, et al. 2017. *Publ. Astron. Soc. Aust.* 34:e058
Espinosa Lara F, Rieutord M. 2012. *Astron. Astrophys.* 547:A32
Evans CJ, Taylor WD, Hénault-Brunet V, et al. 2011. *Astron. Astrophys.* 530:A108
Fabry M, Marchant P, Langer N, Sana H. 2023. *Astron. Astrophys.* 672:A175
Fabry M, Marchant P, Sana H. 2022. *Astron. Astrophys.* 661:A123
Farmer R, Laplace E, de Mink SE, Justham S. 2021. *Ap. J.* 923(2):214
Farmer R, Laplace E, Ma J, et al. 2023a. *Ap. J.* 948(2):111
Farmer R, Renzo M, Götberg Y, et al. 2023b. *MNRAS* 524(2):1692–709
Fellay L, Dupret MA. 2023. *Astron. Astrophys.* 676:A22
Ferrario L, Pringle JE, Tout CA, Wickramasinghe DT. 2009. *MNRAS* 400:L71–74
Fishbach M, Kalogera V. 2022. *Ap. J. Lett.* 929(2):L26
Foellmi C, Moffat AFJ, Guerrero MA. 2003a. *MNRAS* 338(2):360–88
Foellmi C, Moffat AFJ, Guerrero MA. 2003b. *MNRAS* 338(4):1025–56
Fragos T, Andrews JJ, Bavera SS, et al. 2023. *Ap. J. Suppl.* 264(2):45
Fragos T, Andrews JJ, Ramirez-Ruiz E, et al. 2019. *Ap. J. Lett.* 883(2):L45
Fremling C, Miller AA, Sharma Y, et al. 2020. *Ap. J.* 895:32
Frost AJ, Bodensteiner J, Rivinius T, et al. 2022. *Astron. Astrophys.* 659:L3
Frost AJ, Mahy L, Sana H, et al. 2021. In *Proceedings of the MOBSTER-1 Virtual Conference, July 12–17, 2020*, id. 39. Zenodo. **https://doi.org/10.5281/zenodo.5535758**
Fryxell B, Olson K, Ricker P, et al. 2000. *Ap. J. Suppl.* 131:273–334
Fuller J. 2017. *MNRAS* 472(2):1538–64
Gaburov E, Lombardi JC Jr., Portegies Zwart S. 2010. *MNRAS* 402:105–26
Gaia Collab., Brown AGA, Vallenari A, et al. 2021. *Astron. Astrophys.* 649:A1
Gaia Collab., Prusti T, de Bruijne JHJ, et al. 2016. *Astron. Astrophys.* 595:A1
Gallagher JS. 1989. In *Physics of Luminous Blue Variables, IAU Colloq. 113*, ed. K Davidson, AFJ Moffat, HJGLM Lamers, Ap. Space Sci. Libr. 157:185–94. Dordrecht, Neth.: Reidel
Gallegos-Garcia M, Berry CPL, Marchant P, Kalogera V. 2021. *Ap. J.* 922(2):110
Giacobbo N, Mapelli M. 2018. *MNRAS* 480(2):2011–30
Gieren W, Górski M, Pietrzyński G, et al. 2013. *Ap. J.* 773:69
Gies DR, Bagnuolo WG Jr., Ferrara EC, et al. 1998. *Ap. J.* 493:440–50
Gies DR, Shepard K, Wysocki P, Klement R. 2022. *Astron. J.* 163(2):100
Giesers B, Dreizler S, Husser TO, et al. 2018. *MNRAS* 475:L15–19
Giesers B, Kamann S, Dreizler S, et al. 2019. *Astron. Astrophys.* 632:A3
Gilfanov M, Fabbiano G, Lehmer B, Zezas A. 2023. In *Handbook of X-ray and Gamma-ray Astrophysics*, ed. C Bambi, A Santangelo. Singapore: Springer. **https://doi.org/10.1007/978-981-16-4544-0_108-1**
Gilkis A, Shenar T. 2023. *MNRAS* 518(3):3541–55
Gomel R, Faigler S, Mazeh T. 2021. *MNRAS* 501(2):2822–32
Götberg Y, de Mink SE, Groh JH. 2017. *Astron. Astrophys.* 608:A11
Götberg Y, de Mink SE, Groh JH, et al. 2019. *Astron. Astrophys.* 629:A134

Götberg Y, de Mink SE, McQuinn M, et al. 2020. *Astron. Astrophys.* 634:A134
Götberg Y, Drout MR, Ji AP, et al. 2023. *Ap. J.* 959:125
Gou L, McClintock JE, Liu J, et al. 2009. *Ap. J.* 701(2):1076–90
Granada A, Ekström S, Georgy C, et al. 2013. *Astron. Astrophys.* 553:A25
GRAVITY Collab., Karl M, Pfuhl O, et al. 2018. *Astron. Astrophys.* 620:A116
Groh JH, Meynet G, Ekström S. 2013. *Astron. Astrophys.* 550:L7
Guo Z. 2021. *Front. Astron. Space Sci.* 8:67
Haiman Z, Loeb A. 1997. *Ap. J.* 483:21–37
Hainich R, Pasemann D, Todt H, et al. 2015. *Astron. Astrophys.* 581:A21
Hall ED, Evans M. 2019. *Classical Quantum Gravity* 36(22):225002
Han ZW, Ge HW, Chen XF, Chen HL. 2020. *Res. Astron. Astrophys.* 20(10):161
Hannam M, Brown DA, Fairhurst S, et al. 2013. *Ap. J. Lett.* 766:L14
Hannam M, Hoy C, Thompson JE, et al. 2022. *Nature* 610(7933):652–55
Harmanec P, Habuda P, Štefl S, et al. 2000. *Astron. Astrophys.* 364:L85–88
Hastings B, Langer N, Koenigsberger G. 2020a. *Astron. Astrophys.* 641:A86
Hastings B, Langer N, Wang C, et al. 2021. *Astron. Astrophys.* 653:A144
Hastings B, Wang C, Langer N. 2020b. *Astron. Astrophys.* 633:A165
Healy S, Horiuchi S, Colomer Molla M, et al. 2023. arXiv:2307.08785
Heber U. 2009. *Annu. Rev. Astron. Astrophys.* 47:211–51
Heger A, Müller B, Mandel I. 2023. In *The Encyclopedia of Cosmology (Set 2): Frontiers in Cosmology*, Vol. 3, *Black Holes*, ed. Z Haiman, pp. 61–111. New Jersey: World Sci.
Henyey LG, Wilets L, Böhm KH, LeLevier R, Levee RD. 1959. *Ap. J.* 129:628–36
Hillwig TC, Gies DR. 2008. *Ap. J. Lett.* 676:L37–40
Hirai R, Mandel I. 2021. *Publ. Astron. Soc. Aust.* 38:e056
Hirai R, Mandel I. 2022. *Ap. J. Lett.* 937(2):L42
Hirai R, Podsiadlowski P, Owocki SP, et al. 2021. *MNRAS* 503(3):4276–96
Hjellming MS, Webbink RF. 1987. *Ap. J.* 318:794–808
Hobbs G, Lorimer DR, Lyne AG, Kramer M. 2005. *MNRAS* 360(3):974–92
Holgado G, Simón-Díaz S, Herrero A, Barbá RH. 2022. *Astron. Astrophys.* 665:A150
Hopkins PF, Kereš D, Oñorbe J, et al. 2014. *MNRAS* 445:581–603
Horch EP, van Belle GT, Davidson JW Jr., et al. 2020. *Astron. J.* 159(5):233
Hulse RA, Taylor JH. 1975. *Ap. J. Lett.* 195:L51–53
Humphreys RM, Davidson K. 1979. *Ap. J.* 232:409–20
Humphreys RM, Davidson K. 1994. *Publ. Astron. Soc. Pac.* 106:1025
Hurley JR, Pols OR, Tout CA. 2000. *MNRAS* 315(3):543–69
Hurley JR, Tout CA, Pols OR. 2002. *MNRAS* 329(4):897–928
Iorio G, Mapelli M, Costa G, et al. 2023. *MNRAS* 524:426–70
Irrgang A, Geier S, Kreuzer S, et al. 2020. *Astron. Astrophys.* 633:L5
Irrgang A, Przybilla N, Meynet G. 2022. *Nat. Astron.* 6:1414–20
Ivanova N, Chaichenets S, Fregeau J, et al. 2010. *Ap. J.* 717(2):948–57
Ivanova N, Justham S, Chen X, et al. 2013. *Astron. Astrophys. Rev.* 21:59
Izzard RG, Tout CA, Karakas AI, Pols OR. 2004. *MNRAS* 350(2):407–26
Janssens S, Shenar T, Degenaar N, et al. 2023a. *Astron. Astrophys.* 677:L9
Janssens S, Shenar T, Sana H, Marchant P. 2023b. *Astron. Astrophys.* 670:A79
Janssens S, Shenar T, Sana H, et al. 2022. *Astron. Astrophys.* 658:A129
Josselin E, Plez B. 2007. *Astron. Astrophys.* 469(2):671–80
Justham S, Podsiadlowski P, Vink JS. 2014. *Ap. J.* 796(2):121
Kaaret P, Feng H, Roberts TP. 2017. *Annu. Rev. Astron. Astrophys.* 55:303–41
Kalari VM, Horch EP, Salinas R, et al. 2022. *Ap. J.* 935(2):162
Keane E, Bhattacharyya B, Kramer M, et al. 2015. In *Proceeding of Advancing Astrophysics with the Square Kilometre Array (AASKA14)*, *Giardini Naxos*, *Italy*, *June 9–13*, *2014*. *PoS* 14:040
Kervella P, Domiciano de Souza A, Bendjoya P. 2008. *Astron. Astrophys.* 484:L13–16

Keszthelyi Z, Meynet G, Martins F, de Koter A, David-Uraz A. 2021. *MNRAS* 504(2):2474–92
Kiewe M, Gal-Yam A, Arcavi I, et al. 2012. *Ap. J.* 744:10
King AR, Davies MB, Ward MJ, et al. 2001. *Ap. J. Lett.* 552(2):L109–12
Kinugawa T, Inayoshi K, Hotokezaka K, et al. 2014. *MNRAS* 442(4):2963–92
Kippenhahn R, Weigert A. 1967. *Z. Astrophys.* 65:251–73
Klement R, Baade D, Rivinius T, et al. 2022. *Ap. J.* 940:86
Klement R, Carciofi AC, Rivinius T, et al. 2019. *Ap. J.* 885(2):147
Klement R, Hadrava P, Rivinius T, et al. 2021. *Ap. J.* 916:24
Klencki J, Istrate A, Nelemans G, Pols O. 2022. *Astron. Astrophys.* 662:A56
Klencki J, Nelemans G, Istrate AG, Chruslinska M. 2021. *Astron. Astrophys.* 645:A54
Kobulnicky HA, Fryer CL. 2007. *Ap. J.* 670:747–65
Kobulnicky HA, Kiminki DC, Lundquist MJ, et al. 2014. *Ap. J. Suppl.* 213(2):34
Koch DG, Borucki WJ, Basri G, et al. 2010. *Ap. J. Lett.* 713(2):L79–86
Kołaczek-Szymański PA, Pigulski A, Michalska G, et al. 2021. *Astron. Astrophys.* 647:A12
Kolb U, Ritter H. 1990. *Astron. Astrophys.* 236:385–92
Koubský P, Kotková L, Votruba V, et al. 2012. *Astron. Astrophys.* 545:A121
Kramer M, Stairs IH, Manchester RN, et al. 2006. *Science* 314(5796):97–102
Kramer M, Stairs IH, Manchester RN, et al. 2021. *Phys. Rev. X* 11(4):041050
Kroupa P. 2002. *Science* 295(5552):82–91
Kruckow MU, Tauris TM, Langer N, et al. 2018. *MNRAS* 481(2):1908–49
Kuiper GP. 1941. *Ap. J.* 93:133–77
Labadie-Bartz J, Carciofi AC, Henrique de Amorim T, et al. 2022. *Astron. J.* 163(5):226
Lam CY, Lu JR, Udalski A, et al. 2022. *Ap. J. Lett.* 933:L23
Lamb JB, Oey MS, Segura-Cox DM, et al. 2016. *Ap. J.* 817(2):113
Lamers HJGLM, Nugis T. 2002. *Astron. Astrophys.* 395:L1–4
Langer N. 2012. *Annu. Rev. Astron. Astrophys.* 50:107–64
Langer N, Baade D, Bodensteiner J, et al. 2020a. *Astron. Astrophys.* 633:A40
Langer N, Schürmann C, Stoll K, et al. 2020b. *Astron. Astrophys.* 638:A39
Langer N, Wellstein S, Petrovic J. 2003. In *A Massive Star Odyssey: From Main Sequence to Supernova*, *Proc. IAU Symp. 212*, ed. K van der Hucht, A Herrero, C Esteban, pp. 275–80. San Francisco: ASP
Lanthermann C, Le Bouquin JB, Sana H, et al. 2023. *Astron. Astrophys.* 672:A6
Laplace E, Götberg Y, de Mink SE, et al. 2020. *Astron. Astrophys.* 637:A6
Laplace E, Justham S, Renzo M, et al. 2021. *Astron. Astrophys.* 656:A58
Lau MYM, Hirai R, González-Bolívar M, et al. 2022. *MNRAS* 512(4):5462–80
Lauterborn D. 1970. *Astron. Astrophys.* 7:150–59
Laycock SGT, Maccarone TJ, Christodoulou DM. 2015. *MNRAS* 452:L31–35
Le Bouquin JB, Sana H, Gosset E, et al. 2017. *Astron. Astrophys.* 601:A34
Levato H, Malaroda S, Morrell N, Solivella G. 1987. *Ap. J. Suppl.* 64:487–503
Liu J, McClintock JE, Narayan R, et al. 2010. *Ap. J. Lett.* 719:L109
Liu J, Zhang H, Howard AW, et al. 2019. *Nature* 575(7784):618–21
Lombardi JC Jr., Rasio FA, Shapiro SL. 1995. *Ap. J. Lett.* 445:L117–20
Long KS, van Speybroeck LP. 1983. In *Accretion-Driven Stellar X-ray Sources*, ed. WHG Lewin, EPJ van den Heuvel, pp. 117–46. Cambridge/New York: Cambridge Univ. Press
Lucy LB. 1968. *Ap. J.* 151:1123–36
Ma L, Fuller J. 2023. *Ap. J.* 952:53
MacLeod M, Loeb A. 2020. *Ap. J.* 902:85
Maeder A. 1987. *Astron. Astrophys.* 178:159–69
Maeder A, Meynet G. 2000. *Astron. Astrophys.* 361:159–66
Maeder A, Meynet G. 2001. *Astron. Astrophys.* 373:555–71
Mahy L, Lanthermann C, Hutsemékers D, et al. 2022a. *Astron. Astrophys.* 657:A4
Mahy L, Sana H, Abdul-Masih M, et al. 2020. *Astron. Astrophys.* 634:A118
Mahy L, Sana H, Shenar T, et al. 2022b. *Astron. Astrophys.* 664:A159

Maíz Apellániz J, Trigueros Páez E, Negueruela I, et al. 2019. *Astron. Astrophys.* 626:A20
Mandel I, Broekgaarden FS. 2022. *Living Rev. Relativity* 25:1
Mandel I, de Mink SE. 2016. *MNRAS* 458(3):2634–47
Mandel I, Farmer A. 2022. *Phys. Rep.* 955:1–24
Marchant P, Langer N, Podsiadlowski P, et al. 2016. *Astron. Astrophys.* 588:A50
Marchant P, Langer N, Podsiadlowski P, et al. 2017. *Astron. Astrophys.* 604:A55
Marchant P, Pappas KMW, Gallegos-Garcia M, et al. 2021. *Astron. Astrophys.* 650:A107
Marchant P, Renzo M, Farmer R, et al. 2019. *Ap. J.* 882:36
Martayan C, Lobel A, Baade D, et al. 2012. In *Circumstellar Dynamics at High Resolution*, Vol. 464, *ASP Conf. Ser.*, ed. AC Carciofi, T Rivinius, pp. 293–300. San Francisco: ASP
Martayan C, Lobel A, Baade D, et al. 2016. *Astron. Astrophys.* 587:A115
Martins F, Escolano C, Wade GA, et al. 2012. *Astron. Astrophys.* 538:A29
Mashian N, Loeb A. 2017. *MNRAS* 470(3):2611–16
Mason BD, Hartkopf WI, Gies DR, et al. 2009. *Astron. J.* 137(2):3358–77
Mason KO, White NE, Sanford PW. 1976. *Nature* 260:690–91
McCollough ML, Corrales L, Dunham MM. 2016. *Ap. J. Lett.* 830(2):L36
Meilland A, Delaa O, Stee P, et al. 2011. *Astron. Astrophys.* 532:A80
Menon A, Heger A. 2017. *MNRAS* 469:4649–64
Menon A, Langer N, de Mink SE, et al. 2021. *MNRAS* 507(4):5013–33
Metzger BD. 2022. *Ap. J.* 932(2):84
Miller-Jones JCA, Bahramian A, Orosz JA, et al. 2021. *Science* 371(6533):1046–49
Milone AP, Marino AF, Di Criscienzo M, et al. 2018. *MNRAS* 477(2):2640–63
Moe M, Di Stefano R. 2013. *Ap. J.* 778(2):95
Moe M, Di Stefano R. 2017. *Ap. J. Suppl.* 230(2):15
Moreno MM, Schneider FRN, Röpke FK, et al. 2022. *Astron. Astrophys.* 667:A72
Moriya TJ, Mazzali PA, Tominaga N, et al. 2017. *MNRAS* 466(2):2085–98
Mourard D, Brož M, Nemravová JA, et al. 2018. *Astron. Astrophys.* 618:A112
Murase K, Bartos I. 2019. *Annu. Rev. Nucl. Part. Sci.* 69:477–506
Nazé Y, Rauw G, Czesla S, et al. 2022. *MNRAS* 510(2):2286–304
Nazé Y, Rauw G, Hutsemékers D. 2012. *Astron. Astrophys.* 538:A47
Negueruela I. 1998. *Astron. Astrophys.* 338:505–10
Nelson CA, Eggleton PP. 2001. *Ap. J.* 552(2):664–78
Neugent KF. 2021. *Ap. J.* 908:87
Neugent KF, Levesque EM, Massey P. 2018. *Astron. J.* 156(5):225
Neugent KF, Levesque EM, Massey P, Morrell NI. 2019. *Ap. J.* 875(2):124
Neugent KF, Massey P. 2014. *Ap. J.* 789:10
Nieva MF, Przybilla N. 2014. *Astron. Astrophys.* 566:A7
Nomoto K, Kobayashi C, Tominaga N. 2013. *Annu. Rev. Astron. Astrophys.* 51:457–509
O'Connor E, Ott CD. 2011. *Ap. J.* 730(2):70
O'Doherty TN, Bahramian A, Miller-Jones JCA, et al. 2023. *MNRAS* 521(2):2504–24
Okazaki AT, Negueruela I. 2001. *Astron. Astrophys.* 377:161–74
Olejak A, Belczynski K, Ivanova N. 2021. *Astron. Astrophys.* 651:A100
Orosz JA, Steeghs D, McClintock JE, et al. 2009. *Ap. J.* 697:573–91
Oudmaijer RD, Parr AM. 2010. *MNRAS* 405(4):2439–46
Packet W. 1981. *Astron. Astrophys.* 102:17–19
Paczyński B. 1967. *Acta Astron*. 17:355
Paczynski B. 1976. In *Structure and Evolution of Close Binary Systems*, *Proceedings of the Symposium*, *IAU Symp.* 73, ed. P Eggleton, S Mitton, J Whelan, pp. 75–80. Dordrecht, Neth.: Reidel
Paczynski B. 1991. *Ap. J.* 370:597–603
Pasquali A, Nota A, Langer N, et al. 2000. *Astron. J.* 119(3):1352–58
Patrick LR, Lennon DJ, Britavskiy N, et al. 2019. *Astron. Astrophys.* 624:A129
Patrick LR, Lennon DJ, Evans CJ, et al. 2020. *Astron. Astrophys.* 635:A29

Patrick LR, Thilker D, Lennon DJ, et al. 2022. *MNRAS* 513(4):5847–60
Pauli D, Oskinova LM, Hamann WR, et al. 2022. *Astron. Astrophys.* 659:A9
Pauwels T, Reggiani M, Sana H, Rainot A, Kratter K. 2023. *Astron. Astrophys.* 678:A172
Paxton B, Bildsten L, Dotter A, et al. 2011. *Ap. J. Suppl.* 192:3
Paxton B, Marchant P, Schwab J, et al. 2015. *Ap. J. Suppl.* 220:15
Pejcha O, Metzger BD, Tomida K. 2016. *MNRAS* 461(3):2527–39
Peters GJ, Pewett TD, Gies DR, et al. 2013. *Ap. J.* 765:2
Peters PC. 1964. *Phys. Rev.* 136(4B):B1224–32
Petit V, Owocki SP, Wade GA, et al. 2013. *MNRAS* 429:398–422
Pettini M, Steidel CC, Adelberger KL, et al. 2000. *Ap. J.* 528:96–107
Pfahl E, Rappaport S, Podsiadlowski P, Spruit H. 2002. *Ap. J.* 574:364–76
Picco A, Marchant P, Sana H, Nelemans G. 2024. *Astron. Astrophys.* 681:A31
Pietrzyński G, Graczyk D, Gallenne A, et al. 2019. *Nature* 567(7747):200–3
Pietsch W, Haberl F, Sasaki M, et al. 2006. *Ap. J.* 646:420–28
Podsiadlowski P, Joss PC, Hsu JJL. 1992. *Ap. J.* 391:246–64
Podsiadlowski P, Joss PC, Rappaport S. 1990. *Astron. Astrophys.* 227:L9–12
Podsiadlowski P, Langer N, Poelarends AJT, et al. 2004. *Ap. J.* 612(2):1044–51
Poeckert R. 1981. *Publ. Astron. Soc. Pac.* 93:297–317
Pols OR, Cote J, Waters LBFM, Heise J. 1991. *Astron. Astrophys.* 241:419–38
Pols OR, Schröder KP, Hurley JR, et al. 1998. *MNRAS* 298(2):525–36
Popham R, Narayan R. 1991. *Ap. J.* 370:604–14
Portegies Zwart SF, van den Heuvel EPJ. 2016. *MNRAS* 456(4):3401–12
Portegies Zwart SF, Verbunt F. 1996. *Astron. Astrophys.* 309:179–96
Prestwich AH, Kilgard R, Crowther PA, et al. 2007. *Ap. J. Lett.* 669:L21–24
Prša A, Zwitter T. 2005. *Ap. J.* 628:426–38
Qin Y, Fragos T, Meynet G, et al. 2018. *Astron. Astrophys.* 616:A28
Raguzova NV, Popov SB. 2005. *Astron. Astrophys. Trans.* 24(3):151–85
Rainot A, Reggiani M, Sana H, et al. 2020. *Astron. Astrophys.* 640:A15
Ramachandran V, Klencki J, Sander AAC, et al. 2023. *Astron. Astrophys.* 674:L12
Ramachandran V, Oskinova LM, Hamann WR, et al. 2022. *Astron. Astrophys.* 667:A77
Ramírez-Agudelo OH, Sana H, de Mink SE, et al. 2015. *Astron. Astrophys.* 580:A92
Ramírez-Agudelo OH, Simón-Díaz S, Sana H, et al. 2013. *Astron. Astrophys.* 560:A29
Ramírez-Tannus MC, Backs F, de Koter A, et al. 2021. *Astron. Astrophys.* 645:L10
Reggiani M, Rainot A, Sana H, et al. 2022. *Astron. Astrophys.* 660:A122
Reig P. 2011. *Ap. Space Sci.* 332:1–29
Renzo M, Götberg Y. 2021. *Ap. J.* 923(2):277
Renzo M, Zapartas E, de Mink SE, et al. 2019. *Astron. Astrophys.* 624:A66
Ricker GR, Winn JN, Vanderspek R, et al. 2015. *J. Astron. Telescopes Instrum. Syst.* 1:014003
Riley J, Agrawal P, Barrett JW, et al. 2022. *Ap. J. Suppl.* 258(2):34
Ritchie BW, Clark JS, Negueruela I, Najarro F. 2022. *Astron. Astrophys.* 660:A89
Rivinius T, Baade D, Hadrava P, et al. 2020. *Astron. Astrophys.* 637:L3
Rivinius T, Carciofi AC, Martayan C. 2013. *Astron. Astrophys. Rev.* 21:69
Rivinius T, Klement R, Chojnowski SD, et al. 2022. arXiv:2208.12315
Rivinius T, Štefl S, Maintz M, et al. 2004. *Astron. Astrophys.* 427:307–11
Rizzi L, Bresolin F, Kudritzki RP, et al. 2006. *Ap. J.* 638(2):766–71
Rocha KA, Andrews JJ, Berry CPL, et al. 2022. *Ap. J.* 938:64
Romagnolo A, Belczynski K, Klencki J, et al. 2023. *MNRAS* 525:706–20
Röpke FK, De Marco O. 2023. *Living Rev. Comput. Astrophys.* 9:2
Sahu KC, Anderson J, Casertano S, et al. 2022. *Ap. J.* 933:83
Sana H, de Koter A, de Mink SE, et al. 2013. *Astron. Astrophys.* 550:A107
Sana H, de Mink SE, de Koter A, et al. 2012. *Science* 337(6093):444–46
Sana H, James G, Gosset E. 2011. *MNRAS* 416(2):817–31

Sana H, Le Bouquin JB, Lacour S, et al. 2014. *Ap. J. Suppl.* 215:15
Sana H, Ramírez-Agudelo OH, Hénault-Brunet V, et al. 2022. *Astron. Astrophys.* 668:L5
Sana H, Ramírez-Tannus MC, de Koter A, et al. 2017. *Astron. Astrophys.* 599:L9
Saracino S, Kamann S, Guarcello MG, et al. 2022. *MNRAS* 511(2):2914–24
Saracino S, Shenar T, Kamann S, et al. 2023. *MNRAS* 521(2):3162–71
Schaffenroth V, Pelisoli I, Barlow BN, et al. 2022. *Astron. Astrophys.* 666:A182
Schneider FRN, Izzard RG, Langer N, de Mink SE. 2015. *Ap. J.* 805:20
Schneider FRN, Ohlmann ST, Podsiadlowski P, et al. 2019. *Nature* 574(7777):211–14
Schneider FRN, Podsiadlowski P, Langer N, et al. 2016. *MNRAS* 457(3):2355–65
Schneider FRN, Podsiadlowski P, Laplace E. 2023. *Ap. J. Lett.* 950(2):L9
Schneider FRN, Podsiadlowski P, Müller B. 2021. *Astron. Astrophys.* 645:A5
Schnurr O, Moffat AFJ, St-Louis N, et al. 2008. *MNRAS* 389(2):806–28
Schootemeijer A, Götberg Y, de Mink SE, et al. 2018. *Astron. Astrophys.* 615:A30
Schootemeijer A, Langer N. 2018. *Astron. Astrophys.* 611:A75
Schürmann C, Langer N, Xu X, Wang C. 2022. *Astron. Astrophys.* 667:A122
Sen K, Langer N, Marchant P, et al. 2022. *Astron. Astrophys.* 659:A98
Sen K, Langer N, Pauli D, et al. 2023. *Astron. Astrophys.* 672:A198
Sen K, Xu XT, Langer N, et al. 2021. *Astron. Astrophys.* 652:A138
Sesana A. 2016. *Phys. Rev. Lett.* 116(23):231102
Shao Y, Li XD. 2014. *Ap. J.* 796:37
Shapiro SL, Lightman AP. 1976. *Ap. J.* 204:555–60
Shenar T, Bodensteiner J, Abdul-Masih M, et al. 2020a. *Astron. Astrophys.* 639:L6
Shenar T, Gilkis A, Vink JS, et al. 2020b. *Astron. Astrophys.* 634:A79
Shenar T, Hainich R, Todt H, et al. 2016. *Astron. Astrophys.* 591:A22
Shenar T, Sablowski DP, Hainich R, et al. 2019. *Astron. Astrophys.* 627:A151
Shenar T, Sana H, Mahy L, et al. 2022a. *Astron. Astrophys.* 665:A148
Shenar T, Sana H, Mahy L, et al. 2022b. *Nat. Astron.* 6:1085–92
Shenar T, Wade GA, Marchant P, et al. 2023. *Science* 381(6659):761–65
Shu FH, Lubow SH, Anderson L. 1980. *Ap. J.* 239:937–40
Sills A, Adams T, Davies MB, Bate MR. 2002. *MNRAS* 332:49–54
Silverman JM, Filippenko AV. 2008. *Ap. J. Lett.* 678:L17–20
Singh NS, Naik S, Paul B, et al. 2002. *Astron. Astrophys.* 392:161–67
Smith N, Andrews JE, Rest A, et al. 2018. *MNRAS* 480(2):1466–98
Smith N, Tombleson R. 2015. *MNRAS* 447:598–617
Smith RC, Smith DH. 1981. *MNRAS* 194:583–92
Soberman GE, Phinney ES, van den Heuvel EPJ. 1997. *Astron. Astrophys.* 327:620–35
Sota A, Maíz Apellániz J, Morrell NI, et al. 2014. *Ap. J. Suppl.* 211:10
Springel V. 2010. *MNRAS* 401(2):791–851
Springel V, Yoshida N, White SDM. 2001. *New Astron*. 6(2):79–117
Steiner JE, Oliveira AS. 2005. *Astron. Astrophys.* 444(3):895–904
Stone JM, Tomida K, White CJ, Felker KG. 2020. *Ap. J. Suppl.* 249:4
Sukhbold T, Ertl T, Woosley SE, et al. 2016. *Ap. J.* 821:38
Sukhbold T, Woosley SE. 2014. *Ap. J.* 783:10
Sun M, Townsend RHD, Guo Z. 2023. *Ap. J.* 945:43
Taam RE, Sandquist EL. 2000. *Annu. Rev. Astron. Astrophys.* 38:113–41
Tango WJ, Davis J, Jacob AP, et al. 2009. *MNRAS* 396(2):842–48
Tassoul JL, Tassoul M. 1982. *Ap. J.* 261:273–76
Tauris TM, Kramer M, Freire PCC, et al. 2017. *Ap. J.* 846(2):170
Tauris TM, Langer N, Podsiadlowski P. 2015. *MNRAS* 451(2):2123–44
Tauris TM, van den Heuvel EPJ. 2006. In *Compact Stellar X-ray Sources*, Vol. 39, ed. W Lewin, M van der Klis, pp. 623–65. Cambridge, UK: Cambridge Univ. Press
Tauris TM, van den Heuvel EPJ. 2023. *Physics of Binary Star Evolution. From Stars to X-ray Binaries and Gravitational Wave Sources*. Princeton, NJ: Princeton Univ. Press

Taylor JH, Fowler LA, McCulloch PM. 1979. *Nature* 277(5696):437–40
Temmink KD, Pols OR, Justham S, et al. 2023. *Astron. Astrophys.* 669:A45
Thorne KS, Zytkow AN. 1975. *Ap. J. Lett.* 199:L19–24
Trigueros Páez E, Barbá RH, Negueruela I, et al. 2021. *Astron. Astrophys.* 655:A4
Tutukov AV, Yungelson LR. 1993. *MNRAS* 260:675–78
Ugliano M, Janka HT, Marek A, Arcones A. 2012. *Ap. J.* 757:69
Valsecchi F, Glebbeek E, Farr WM, et al. 2010. *Nature* 468(7320):77–79
van Bever J, Vanbeveren D. 1997. *Astron. Astrophys.* 322:116–26
van den Heuvel EPJ. 1976. In *Structure and Evolution of Close Binary Systems*, *Proceedings of the Symposium*, *IAU Symp.* 73, ed. P Eggleton, S Mitton, J Whelan, pp. 35–61. Dordrecht, Neth.: Reidel
van den Heuvel EPJ, Portegies Zwart SF, de Mink SE. 2017. *MNRAS* 471(4):4256–64
van der Hucht KA. 2001. *New Astron. Rev.* 45(3):135–232
van Son LAC, de Mink SE, Chruślińska M, et al. 2023. *Ap. J.* 948(2):105
Vanbeveren D. 2012. In *Four Decades of Massive Star Research—A Scientific Meeting in Honor of Anthony F. J. Moffat*, Vol. 465, *ASP Conf. Ser.*, ed. L Drissen, C Robert, N St-Louis, AFJ Moffat, pp. 342–47. San Francisco: ASP
Vanbeveren D, Conti PS. 1980. *Astron. Astrophys.* 88:230–39
Vanbeveren D, De Donder E, Van Bever J, et al. 1998. *New Astron.* 3(7):443–92
Vanbeveren D, Mennekens N, van den Heuvel EPJ, Van Bever J. 2020. *Astron. Astrophys.* 636:A99
Varma V, Biscoveanu S, Islam T, et al. 2022. *Phys. Rev. Lett.* 128(19):191102
Verbunt F, Phinney ES. 1995. *Astron. Astrophys.* 296:709–21
Vigna-Gómez A, Liu B, Aguilera-Dena DR, et al. 2022. *MNRAS* 515:L50–55
Vigna-Gómez A, Neijssel CJ, Stevenson S, et al. 2018. *MNRAS* 481(3):4009–29
Villaseñor JI, Lennon DJ, Picco A, et al. 2023. *MNRAS* 525(4):5121–45
Villaseñor JI, Taylor WD, Evans CJ, et al. 2021. *MNRAS* 507(4):5348–75
Vinciguerra S, Neijssel CJ, Vigna-Gómez A, et al. 2020. *MNRAS* 498(4):4705–20
Vink JS. 2022. *Annu. Rev. Astron. Astrophys.* 60:203–46
von Zeipel H. 1924. *MNRAS* 84:665–83
Wang C, Langer N, Schootemeijer A, et al. 2020. *Ap. J. Lett.* 888:L12
Wang C, Langer N, Schootemeijer A, et al. 2022. *Nat. Astron.* 6:480–87
Wang L, Gies DR, Peters GJ. 2018. *Ap. J.* 853(2):156
Wang L, Gies DR, Peters GJ, et al. 2021. *Astron. J.* 161(5):248
Wang L, Gies DR, Peters GJ, Han Z. 2023. *Astron. J.* 165(5):203
Webbink RF. 1984. *Ap. J.* 277:355–60
Weisberg JM, Nice DJ, Taylor JH. 2010. *Ap. J.* 722(2):1030–34
Wellstein S, Langer N, Braun H. 2001. *Astron. Astrophys.* 369:939–59
Welsh WF, Orosz JA, Aerts C, et al. 2011. *Ap. J. Suppl.* 197:4
Wiktorowicz G, Wyrzykowski Ł, Chruslinska M, et al. 2019. *Ap. J.* 885:1
Willcox R, MacLeod M, Mandel I, Hirai R. 2023. *Ap. J.* 958:138
Witte MG, Savonije GJ. 1999. *Astron. Astrophys.* 350:129–47
Yalinewich A, Beniamini P, Hotokezaka K, Zhu W. 2018. *MNRAS* 481:930–37
Yamaguchi MS, Kawanaka N, Bulik T, Piran T. 2018. *Ap. J.* 861:21
Yoon SC, Woosley SE, Langer N. 2010. *Ap. J.* 725:940–54
Zahn JP. 1975. *Astron. Astrophys.* 41:329–44
Zahn JP. 2008. In *Tidal Effects in Stars, Planets and Disks*, Vol. 29, *EAS Publ. Ser.*, ed. MJ Goupil, JP Zahn, pp. 67–90. Les Ulis, Fr.: EDP Sci.
Zdziarski AA, Mikolajewska J, Belczynski K. 2013. *MNRAS* 429:L104–8
Zevin M, Bavera SS, Berry CPL, et al. 2021. *Ap. J.* 910(2):152